

## Supporting Information for Monovalent SARS-COV-2 mRNA vaccine using optimal UTRs and LNPs is highly immunogenic and broadly protective against Omicron variants

Zhongfeng Ye <sup>a,†</sup>, Srinivasa Reddy Bonam <sup>b,†</sup>, Lindsay G. A. McKay <sup>c</sup>, Jessica A. Plante <sup>b,d</sup>, Jordyn Walker <sup>b,d</sup>, Yu Zhao <sup>a</sup>, Changfeng Huang <sup>a</sup>, Jinjin Chen <sup>a</sup>, Chutian Xu <sup>a</sup>, Yamin Li <sup>e</sup>, Lihan Liu <sup>a</sup>, Joseph Harmon <sup>a</sup>, Shuliang Gao <sup>a</sup>, Donghui Song <sup>a</sup>, Zhibo Zhang <sup>a</sup>, Kenneth S. Plante <sup>b,d</sup>, Anthony Griffiths <sup>c</sup>, Jianzhu Chen <sup>f</sup>, Haitao Hu <sup>b,\*</sup>, Qiaobing Xu <sup>a,\*</sup>

<sup>a</sup> Department of Biomedical Engineering, Tufts University, 4 Colby Street, Medford, MA 02155, USA.

<sup>b</sup> Department of Microbiology and Immunology, University of Texas Medical Branch, 301 University Blvd, Galveston, TX 77555, USA

<sup>c</sup> National Emerging Infectious Diseases Laboratories (NEIDL) and Department of Virology, Immunology, and Microbiology, Chobanian & Avedisian School of Medicine, Boston University, 620 Albany Street, Boston, MA 02215, USA

<sup>d</sup> World Reference Center for Emerging Viruses and Arboviruses, University of Texas Medical Branch, Galveston, TX, USA 77555

<sup>e</sup> Department of Pharmacology, State University of New York Upstate Medical University, Syracuse, New York 13210, USA

<sup>f</sup> Koch Institute for Integrative Cancer Research and Department of Biology, Massachusetts Institute of Technology, Cambridge, MA 02139, USA

† These authors contributed equally to this work

Corresponding author: Qiaobing Xu & Haitao Hu  
Email: Qiaobing.Xu@tufts.edu (Q.X.); haihu@utmb.edu (H.H.)

### This PDF file includes:

Supplementary Methods and Materials  
Figures S1 to S22  
Tables S1 to S6

## Supplementary Methods and Materials

### Cell Culture.

HEK293 and HeLa cells were grown in an Eagle's complete Dulbecco's modified medium (DMEM) supplemented with 10% fetal bovine serum (Sigma-Aldrich), 100 U/mL of penicillin, and 0.1 mg/mL of streptomycin (Sigma-Aldrich).

### Generation of plasmids

**pcDNA3.0-5'UTRs-eGFP-3'UTRs.** S27a-45', NCA, 70nt, Ces1d 5'UTR single strand DNA fragments were ordered from Integrated DNA Technologies (IDT) (**Table S2**). These sequences were amplified and introduced into upstream of eGFP by PCR using primers A216-A225 (**Table S4**). Four plasmids (pcDNA3.0-S27a-45'-eGFP, pcDNA3.0-NCA-eGFP, pcDNA3.0-70nt-eGFP and pcDNA3.0-Ces1d-eGFP) were obtained. Thirteen 3' UTR fragments of interest were chemically synthesized from IDT including  $\alpha$ -globin, MS10433, Apolipoprotein A-II (Apo A-II), Cytochrome P450 2E1 (P450 2E1), Complement Component 3 (C3), YY2 Transcription Factor (YY2 TF), TIAM1, FAM171A1, AP3B1, OXR1, POTEE, WIPI2, S0\_M\_T1012 (**Table S3**), and were introduced into 3'UTR of pcDNA3.0-Ces1d-eGFP and pcDNA3.0-70nt-eGFP in PCR reactions with primers A333 and A334 (**Table S4**).

**pMRNA-Ces1d-Fluc-eGFP-3'UTRs and pMRNA-70nt-Fluc-eGFP-3'UTRs.** The coding sequence for a fused reporter gene, enhanced green fluorescent protein (eGFP) and firefly luciferase (Fluc), was amplified using PCR. The resulted Fluc-eGFP (Luc-GFP) fusion gene was then inserted into a pMRNAxp vector (System Biosciences, US) using primers A164/A165 (**Table S4**). The original 5'UTR ( $\alpha$ -globin) of pMRNA-Luc-GFP were then substituted with Ces1d or 70nt to generate pMRNA-Ces1d-Luc-GFP or pMRNA-70nt-Luc-GFP plasmids using primer A222/A223 or A224/A225, respectively. In pMRNA-Ces1d-Luc-GFP-3'UTRs, Mm $\beta$ -globin,  $\alpha$ -globin, C3, TIAM1, P450 2E1, AP3B1 and WIPI2 were introduced into 3'UTRs. In pMRNA-70nt-Luc-GFP-3'UTRs, Mm $\beta$ -globin, MS10433, Apo A-II,  $\alpha$ -globin, AP3B1, POTEE, S0\_M\_T1022, YY2 TF and OXR1 were introduced into 3'UTRs.

**pMRNA-SARS-2-S and its variants.** Mammalian-codon-optimized SARS-CoV-2 S gene (SARS-2-S) were PCR amplified from pUC57-2019-nCoV-S(Human) plasmid (GenScript) and introduced into pMRNAxp vector (System Biosciences) or UTRs optimized pMRNA using primer A115/A116. Similarly, SARS-CoV-2 truncated S gene (SARS-2-tS) without transmembrane domain was introduced into linearized pMRNAxp with primers A146/A172. Based on the pMRNA-SARS-2-S and pMRNA-SARS-2-tS plasmids, we cloned mutated versions with alterations at the S1/S2 furin cleavage site (-PRRAR/S-). We generated SARS-2-S<sub>delta</sub> and SARS-2-tS<sub>delta</sub> variants by deleting multibasic motif (three arginine in 682, 683 and 685 position) in the furin cleavage site of SARS-2-S and SARS-2-tS. These two variants were obtained by three step PCR using mutagenic complementary pairs of primers, A146/A175 and A160/A175 and A146/A160 (**Table S4**). For pMRNA-SARS-2-S<sub>pp</sub> generation, SARS-CoV-2 Spike gene with two proline substitution at residues 986 and 987 was also generated using mutagenic complementary primers in which A159 and A161 primers carry two proline codons marked in red (**Table S4**). The gene with homolog arms was fused with linearized pMRNAxp using a Cold Fusion Kit (System Biosciences).

**pMRNA-Ces1d-S<sub>pp</sub>-AP3B1 and pMRNA-70nt-S<sub>pp</sub>-Apo A-II.** S<sub>pp</sub> was PCR amplified and introduced into pMRNA-Ces1d-Ap3B1 and pMRNA-70nt-Apo A-II vectors by primers A368/A369 and A370/A371. For pMRNA-70nt-Apo A-II, we constructed two format, including pMRNA-70nt(GG)-Apo A-II and pMRNA-70nt(AG)-Apo A-II, and their UTR sequences were shown in **Table S2**. Their mRNA format from these two constructs is capped with ARCA cap for GG start and CleanCap for AG start, respectively.

### **mRNA synthesis**

The pMRNA-Luc-GFP or pMRNA-S variants plasmid was used as template for gene polyadenylation using the Tail PCR Primer A93/A95, of which reverse primer contains 120 oligodT (**Table S4**). The Tail PCR product after DNA gel purification was used as template in an *in vitro* transcription reaction (10×T7 reaction buffer (1×), CleanCap AG or ARCA cap (10 mM), ATP (10 mM), CTP (10 mM), GTP (3.75 mM), N1-methylpseudouridine (N1mψ, 3.75 mM), each of mRNA templates (25 ng/μL), and T7 RNA polymerase mix) and treated with Turbo DNase (ThermoFisher) and Antarctic Phosphatase (New England Biolabs) and purified using a MegaClear Kit (Life Technologies). The modified nucleotide N1mψ (TriLink) were used to completely substitute their natural counterparts UTP in mRNA synthesis.

### **Plasmid pcDNA3.0-5'UTR-eGFP-3'UTR transfection**

HEK293 cells were seeded into a 48-well plate in DMEM at a concentration of 20,000 cells per well. 0.5 μg of each plasmid was mixed with lipofectamine 2,000 (LPF2k) at a weight ratio of 1:1 and added into each of the wells. 24 hrs post-transfection, the cell media were replaced with fresh DMEM to reduce LPF2k derived cell toxicity. Flow cytometry was performed at each time point post transfection.

### **SARS-CoV-2 Spike mRNA *in vitro* transfection**

HEK293 or HeLa cells were seeded in a 24-well plate at 200,000 cells/well. 18 hrs later, the cells were transfected with spike or modified spike mRNAs (2.4 μg/well) using LPF2k. 5.5 hrs later, the medium was replaced with 200 μL Opti-MEM™ (Reduced Serum Medium). The supernatant was collected at 48 hrs after transfection, centrifugated at 10,500 xg, 1 min to remove cell debris, and then mixed with 4× SDS loading buffer (non-reducing). The residual cell was treated with 100 μL 20 mM HEPES containing 1% Triton-X 100 and 1x proteinase inhibitor (Sigma-Aldrich). Cell lysate from each sample was collected in 1.5 mL tubes and debris was removed by centrifugation under 8,000 xg for 1.5 min. Each sample was mixed with NuPage LDS sample buffer (4x) at 3:1 ratio and then loaded on SDS-PAGE without heating. The spike proteins in both medium and cell lysate were then detected using Western blot with a monoclonal antibody (mAb) against the SARS-CoV-2 S1 protein (Sino Biological).

### **Western blotting analysis**

Unless specified otherwise, 25 μg total proteins were separated on a 4–12% bis-tris polyacrylamide gel (Thermo Fisher Scientific) in MOPS buffer (Thermo Fisher Scientific) at condition, 120 voltage, 58 min. The gel was transferred onto a PVDF membrane and blotted with SARS-CoV-2 (2019-

nCoV) Spike Neutralizing Antibody (Sino Biological) at 1:500 dilution. Anti-mouse secondary antibodies (Abcam) with Horseradish Peroxidase (HRP) were applied to primary antibody at 1:10,000 dilution. HRP conjugated antibody against GAPDH (Thermo Scientific) at 1:2,000 dilution was used to label GAPDH. After washing, equal volume of immobilon dye (Millipore Sigma) was mixed together and applied to sample membrane. The photo of the stained membrane was taken under imager Chemi series with 30 sec exposure.

### **ALC-0315, 113O12B and Lipid 88 synthesis and characterization**

ALC-0315 and 113O12B were synthesized according to our published procedure (1). Lipid 88 was synthesized through Michael addition (**Fig. S3A**). 3,3'-Diamino-N-methyldipropylamine (amine head 306), and an acrylate tail 88 (5 eq.) were mixed in a Teflon-lined glass screw-top vial and heated at 70 °C for 48 h. The crude products were then purified by a Teledyne Isco Chromatography system using methanol/DCM as mobile phase. The fractions containing the desired products which were checked by TLC and ESI-MS were pooled and concentrated to afford lipid 88.

### **LNP88 formulation screening in mice via S.C. route**

All procedures for the animal experiments were approved by the Tufts University Institutional Animal Care and Use Committee (IACUC) and performed in accordance with the National Institutes of Health (NIH) guidelines for the care and use of experimental animals. To optimize LNP88 formulation, we used 5 µg Fluc mRNA (mLuc, TriLink BioTechnologies) as a model cargo. Levels of FLuc expression were evaluated using the IVIS imaging system. Lipid88, cholesterol, DSPC, and DMG-PEG were all dissolved in 100% ethanol at 10 mg/mL. Lipid mixture in a series of weight ratios was added to a triple volume of 25 mM sodium acetate buffer (pH 5.2) dropwise, respectively. Formulated LNPs were dialyzed with a ThermoScientific Slide-ALyzer MINI dialysis device (3.5 K MWCO) overnight. Weight ratios of LNP88 at 16:8:4:3 (lipid88: cholesterol: DSPC: DMG-PEG) were chosen for later UTR optimization via the S.C. route. The concentration of active lipids reached 1.3 µg/µL. The mRNA was then encapsulated into LNP prior to delivery in mice (see mRNA transfection in Experiment section). The hydrodynamic size and polydispersity of LNPs were measured by dynamic laser scattering (DLS) analysis.

### ***In vivo* UTRs screening via S.C. route**

BALB/c mice (4–6 weeks old) were injected with LNP88 containing 5 µg Luc-GFP mRNA with different UTR pairs (mLuc-GFP) and 50 µg active lipid with S.C. injection at the tail base. 6 hrs or 30 hrs after the injection, 0.1 mL of D-Luciferin, at a concentration of 15 mg/mL, was intraperitoneally injected into the mice. 10 min later, the mice were imaged using the *In vivo* Imaging System (PerkinElmer). The radiance of bioluminescence in mice was obtained.

### **LNP88 formulations screening in mice via I.M. route**

LNP88 formulations (lipid88: Chol: DSPC: DMG-PEG) were pre-prepared using the ratio from 16:7.44:3.35:1.86 to 16:8:5:3. At 6 hrs, 24 hrs, 48 hrs and 80 hrs after the injection of the mLuc-LNP88, BALB/c mice were injected intraperitoneally with 0.1 mL D-Luciferin (15 mg/mL in PBS)

and imaged using IVIS. Bioluminescence was quantified using the Living Image software (PerkinElmer).

### **Transmission Electron Microscope (TEM)**

TEM characterization was performed with a FEI Technai Spirit Transmission Electron Microscope (CNS, Harvard University). To prepare the TEM sample, 15  $\mu$ L sample solution was dropped onto a carbon-coated copper grid for 10-15 min and blotted with filter paper to remove excess liquid. Then the sample was negatively stained with 20% Uranyl acetate for 1-2 min, blotted again and air-dried before analysis on TEM.

### **LNP88/Cre mRNA delivery in Ai14D mice.**

Ai14D mice were administered with LNP88 containing Cre mRNA (TriLink) (0.5 mg/kg mRNA per mouse) via I.M. injection. At day 4 and day 15 post LNP-mCre nanocomplex delivery, the spleen and lymph node were collected and homogenized in ACK buffer and filtered through a 70- $\mu$ m strainer (Corning). The splenocytes and lymphocytes were centrifuged at 1,500  $xg$  for 5 min and the cell pellets were resuspended in flow cytometry staining buffer (eBioscience). Then  $2 \times 10^6$  cells were incubated with DAPI and fluorophore-conjugated antibodies of interest listed in **Table S5** with all 1:50 (v/v) dilution at dark 4°C for 1 hr. After washing once with staining buffer, the cells were analyzed using Attune flow cytometer (BD Biosciences). Data was collected and analyzed by FlowJo-v10. Gating information is shown in **Fig. S13**.

### **Mouse immunization and tissue collection**

Vaccine immunogenicity and efficacy were evaluated in 6-week-old female C57BL6 (the Jackson Laboratory; strain no: 000664). For immunogenicity, five groups of mice (n=5) were immunized intramuscularly with either mock (PBS), TU88mCSA, TU88mrS, ALCmCSA, and ALCmrS at week 0 (prime) and week 3 (boost), respectively. 50  $\mu$ L of each vaccine was injected in the right thigh of mice. Blood and serum were collected at week 2 post booster for quantifying antibody titer. Soon after blood collection, mice were euthanized to collect spleen and lung. IgG and IgA antibodies titer were further examined in mouse bronchoalveolar lavage fluid (BALF) to evaluate the immune response at respiratory tract. Afterwards, vaccine-induced cellular immune responses can be analyzed in spleen and lung using immunostaining.

### **Enzyme-linked immunosorbent assay (ELISA)**

For antibody detection, groups of BALB/c mice were immunized with different vaccines on days 0 and 21. At day 26, 200  $\mu$ L of blood was drawn from the facial vein, and levels of antigen-specific IgG in the serum were measured by ELISA. For ELISA, flat-bottomed 96-well plates were precoated with spike protein at a concentration of 2  $\mu$ g/mL protein per well in 100 mM carbonate buffer (pH 9.6) at 4°C overnight. After five TBS-T (TBS-0.1% Tween20) washes, plates with coating protein were then blocked with 3% BSA in PBS. Serum from immunized animals was diluted 100 times in TBS-T, pH 7.4, added to the wells and incubated at 37°C for 2 hrs. Following five times TBS-T washes, horseradish peroxidase (HRP)-conjugated goat anti-mouse IgG (#7076, Cell Signaling) was used at a dilution of 1:10,000 in TBS-T (1% BSA) for labeling. Following 1 hr incubation, the

plates were washed with TBS-T for another 5 times. 100  $\mu$ L TMB was added to each well. After 30 sec incubation, 100  $\mu$ L stop solution (0.16 M sulfuric acid) was immediately added to each well. The blue color of TMB changed to yellow, which was detected by 450 nm UV absorbance.

### **Immunostaining in spleen and lung immune cells**

Total lung tissues were harvested from mock and vaccinated mice. Further, lung tissues were minced, and digested with 0.05% collagenase type IV (Gibco/Thermo Fisher Scientific) in Dulbecco's Modified Eagle's Medium (DMEM, Sigma-Aldrich) for 30 min at 37°C. Lung single-cell suspensions were made by passing lung homogenates through 70- $\mu$ m cell strainers. Similarly, splenocytes were harvested with the 3 mL syringe plunger by gently rupturing the tissue. Spleen single-cell suspensions were made by passing tissue through a 70- $\mu$ m strainer. In both homogenates, red blood cells were removed using red cell lysis buffer (Sigma-Aldrich). Leukocytes were stained with the Fixable Viability Dye (eFluor 506) (eBioscience/Thermo Fisher Scientific) for live/dead cell staining, blocked with 10% FCS in FACS buffer, and stained with fluorochrome-labeled antibodies (Abs). The following antibodies were used to surface stained the cells. CD45.2-PE/Cyanine7, CD4-APC/Fire™ 750, CD8a-Brilliant Violet 570™, CD44-PerCP, CD69-FITC, CD186 (CXCR6)-Brilliant Violet 711™, CD19-PE/Fire™ 640, and CD3-APC (clone and catalogue information can be found at **Table. S6**). The surface staining was performed on ice for 30 min. Cells were then washed with Perm/Wash buffer and resuspended with FACS buffer. To detect RBD-specific B cells, we incubated recombinant RBD proteins coupled with allophycocyanin (APC) with the cells for 30 min at 4°C. RBD-APC positive B cells were identified as RBD<sup>+</sup> B cells. To detect S<sub>539-546</sub> epitope-specific CD8<sup>+</sup> T cells, we incubated PE-labelled SARS-CoV-2 S<sub>539-546</sub> major histocompatibility complex class I tetramer (H-2Kb) [National Institutes of Health (NIH) Tetramer Core] with the cells for 30 min at 4°C. CD44<sup>+</sup> tetramer-positive CD8<sup>+</sup> T cells were identified as S<sub>539-546</sub> epitope-specific CD8<sup>+</sup> T cells. After surface and viability staining, cells were fixed with fixation buffer (BioLegend, 420801) on ice for 20 min. Cells were then washed with perm/wash buffer and were processed with a multiparametric flow cytometer FACS LSRFortessa (BD Biosciences). Data were analyzed using FlowJo (TreeStar).

### **SARS-CoV-2 WA1/2020 and Omicron BA.1 challenge study in hamsters**

All experiments were performed in the Biosafety Level 4 laboratory of the National Emerging Infectious Diseases Laboratories (NEIDL) of Boston University. Cell culture was performed as following: NR-596 Vero E6 cells were maintained in high glucose DMEM (Gibco) supplemented with 1X GlutaMAX, 1 mM sodium pyruvate, 10% FBS (Gibco) and 1X non-essential amino acids (Gibco). Cells were seeded into 6-well plates at a density of  $8.0 \times 10^5$  cells per well. The cells were incubated at 37°C and 5% CO<sub>2</sub> overnight.

The *in vivo* hamster study was performed as following: The experimental design is visually detailed in **Fig. 4A** and *SI Appendix, Fig. S18*. 32 golden Syrian hamsters were divided into 8 groups: groups 1-4 were challenged intranasally with SARS-CoV-2 WA/2020, groups 5-8 were challenged I.N. with SARS-CoV-2 Omicron BA.1 and were either vaccinated with saline (mock control) or with the test article. Groups 2, 4, 6 and 8 were euthanized at 4 DPI for viral lung titers and groups 1, 3, 5 and 7 were monitored for weight on a daily basis for up to 14 DPI.

On Day 30, each animal was challenged with  $4 \times 10^5$  PFU/mL of WA/2020 ( $4 \times 10^4$  PFU/100  $\mu$ L) or  $1.3 \times 10^5$  PFU/mL BA.1 ( $1.3 \times 10^4$  PFU/100  $\mu$ L). Daily weights were taken for each animal up until day 44 when all remaining animals were euthanized, and lung tissue was harvested after euthanasia at day 34 from the relevant groups for quantifying viremia via crystal violet plaque assay (*SI Appendix, Fig. S18B*).

The lung titer plaque assays were performed as following: From each lung sample, a 100 mg portion was cut. This was then transferred to a 2 mL tube and homogenized to a total volume of 1 mL DMEM (Gibco, supplemented with 2% FBS) using a 5 mm stainless steel bead and a Tissuelyser II. Homogenization was carried out at 30 Hz for 2 min, repeated twice. The homogenized tissue was clarified by centrifugation and the lung viral titer was quantified using crystal violet plaque assay. Plaque assays were carried out by first diluting the homogenized lung tissue in DMEM (Gibco) supplemented with 1x GlutaMAX, 1 mM sodium pyruvate, 10% FBS (Gibco) and 1x non-essential amino acids (Gibco) and 200  $\mu$ L of each dilution was added to the confluent monolayers of NR-596 Vero E6 cells (ATCC# C1008) in duplicate and incubated in a 5% CO<sub>2</sub> incubator at 37°C for 1 hr. The cells were rocked gently every 10-15 min to prevent monolayer drying. Cells were then overlaid with a 1:1 solution of 2.5% (v/v) Avicel® RC-591 microcrystalline cellulose and carboxymethylcellulose sodium (DuPont Nutrition & Biosciences) and 2x Modified Eagle Medium (MEM-Temin's modification, Thermo Fisher Cat# 10370088) supplemented with 100x antibiotic-antimycotic (Thermo Fisher Scientific Cat# 15240062) and 100x GlutaMAX both to a final concentration of 2x, and 10% (v/v) FBS. The plates were then incubated at 37°C for two days (WA/2020) or four days (BA.1). After two or four days, the monolayers were fixed with 10% (v/v) neutral buffered formalin (NBF) (Fisher Sci Cat# LC146705) for at least 6 hrs and stained with 0.2% (v/v) aqueous Gentian Violet (Fisher Sci Cat# 3233-16) in 10% (v/v) NBF for 30 min, followed by rinsing and plaque counting.

### **Hamster immunization and SARS-CoV-2 Omicron BQ.1 challenge**

All experiments were performed in the Biosafety Level 3 laboratory at University of Texas Medical Branch, Galveston. Vaccine-induced protection against BQ.1 was evaluated in hamsters. Three groups of 4-5 weeks-old male golden Syrian hamsters (5 per group) I.M. vaccinated with PBS (mock control), ALCmCSA (5  $\mu$ g) or TU88mCSA (5  $\mu$ g). The vaccine or control was administered at 150  $\mu$ L per injection. Serum samples were collected from all hamsters before viral challenge to measure vaccine-induced binding and neutralizing antibodies. Two weeks after booster vaccination (at week 5), hamsters were transferred to the animal biosafety level 3 facility and I.N. challenged with the Omicron BQ.1 strain ( $2 \times 10^4$  pfu; World Reference Center for Emerging Viruses and Arboviruses). On 2 DPI, five hamsters challenged with Omicron BQ.1 were euthanized. Nasal wash samples and portions of the lung tissues were collected for various analyses of vaccine-induced protection. On 4 DPI, the same procedures were repeated for the half of hamsters in each group (five for Omicron). Hamster body weights were monitored daily to evaluate vaccine-induced protection from body weight loss.

### **RNA extraction and RT-PCR quantification of viral RNA copies**

The TRIzol LS Reagent (Thermo Fisher Scientific) was used to extract RNA from lung tissues (mice and hamsters) and nasal washes (hamsters), according to the manufacturer's instructions. One-step RT-PCR was used to quantify SARS-CoV-2 viral RNA copies using the iTaq Universal SYBR Green One-Step Kit (Bio-Rad) and the CFX Connect Real-Time PCR Detection System (Bio-Rad). The SARS-CoV-2 E gene primer sets (forward, 5'-GGAAGAGACAGGTACGTTAATA-3'; reverse, 5'-AGCAGTACGCACACAATCGAA-3') were utilized. Primers (10 M), RNA sample (2 µL), iTaq universal SYBR Green reaction mix (2x; 10 µL), iScript reverse transcriptase (0.25 µL), and molecular grade water were used in PCR reactions (20 µL). The following PCR cycling conditions were used: 95°C for 3 min, 45 cycles of 95°C for 5 s, and 60°C for 30 s. A standard curve (in vitro transcribed, 3839 base pairs encompassing genomic nucleotide positions 26,044 to 29,883 of the SARS-CoV-2 genome) was added in each RT-PCR to measure the absolute copies of viral RNA in lung tissue or nasal wash.

### **Omicron BQ.1 challenge model**

All experiments were performed in the Biosafety Level 3 laboratory at University of Texas Medical Branch, Galveston. Vaccine-induced protection against BQ.1 was evaluated in hamsters. Three groups of 4-5 weeks-old male golden Syrian hamsters (5 per group) I.M. vaccinated with PBS (mock control), ALCmCSA (5 µg) or TU88mCSA (5 µg). The vaccine or mock control group was administered at 150 µL per injection. Serum samples were collected from all hamsters before viral challenge to measure vaccine-induced binding and neutralizing antibodies. Two weeks after booster vaccination (at week 5), hamsters were transferred to the animal biosafety level 3 facility and I.N. challenged with the Omicron BQ.1 strain ( $2 \times 10^4$  pfu; World Reference Center for Emerging Viruses and Arboviruses). On 2 DPI, five hamsters challenged with Omicron BQ.1 were euthanized. Nasal wash samples and portions of the lung tissues were collected for various analyses of vaccine-induced protection. On 4 DPI, the same procedures were repeated for the half of hamsters in each group (five for BQ.1). Hamster body weights were monitored daily to evaluate vaccine-induced protection from body weight loss.

### **Plaque assay in Omicron BQ.1 challenge model**

Nasal washes or homogenized lung tissues were serially diluted in DMEM with 1% antibiotic-antimycotic (Gibco) and allowed to infect a confluent monolayer of Vero E6 cells (ATCC; CRL-1586) on a 96-well plate for 45 min at 37°C with 5% CO<sub>2</sub>. Following infection, cells were treated with an 85% MEM (Gibco) and 15% DMEM solution supplemented with 1% antibiotic-antimycotic and 0.85% methyl cellulose (Sigma-Aldrich). The monolayers were fixed with formalin (Thermo Fisher Scientific) for at least 24 hrs after 36 hrs. Monolayers were rinsed with DPBS (Sigma) and treated for 30 min at room temperature in permeabilization buffer consisting of DPBS supplemented with 0.1% bovine serum albumin (Sigma-Aldrich) and 0.1% saponin (Sigma-Aldrich). Permeabilization buffer was withdrawn, and monolayers were treated overnight at 4°C with rabbit polyclonal antibody diluted in permeabilization buffer (1:3000) against SARS-CoV N protein. Excess antibody was removed with DPBS before incubating monolayers for 1 hour at room temperature with HRP-conjugated goat anti-rabbit IgG (Cell Signaling Technology, 7040) diluted in permeabilization buffer (1:2000). Excess antibody was removed with DPBS before staining foci with KPL TrueBlue Peroxidase Substrate (SeraCare). Excess substrate was removed, and the monolayers were



rinsed with water once foci were visible under a light microscope. The Cytation7 Imaging Reader (BioTek) was used to image the wells. The foci were manually counted, and the findings were shown as focus-forming units (FFU).

## Statistics

Statistical analysis was performed using Tukey's or Šídák's multiple comparisons test in GraphPad Prism version 9.0.0 (GraphPad Software). \*P < 0.05 was considered statistically significant. \*\*P < 0.05 and \*\*\*P < 0.005 \*\*\*\*P < 0.0001 were considered highly significant.

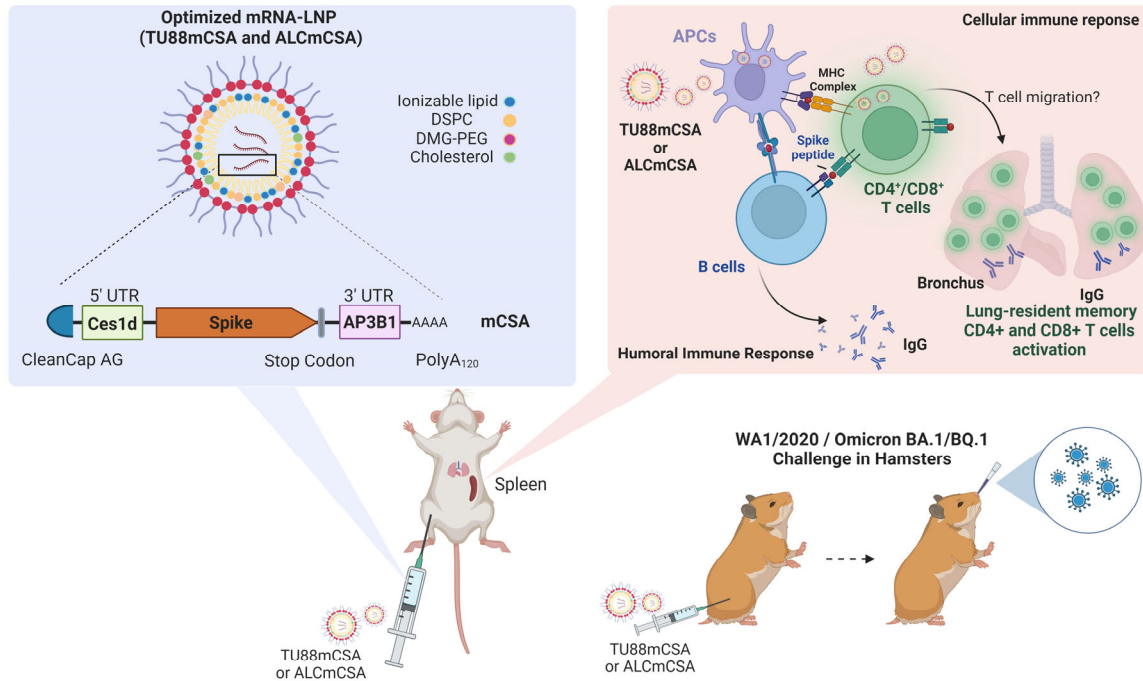


**Fig. S1. Schematic illustration of the development of broad spectrum COVID-19 mRNA vaccine.** mRNA constructs using the ancestral spike gene sequence were prepared with optimized 5'UTR and 3'UTR sequences (5'UTR-Ces1d-Ap3B1-3'UTR) with high translation efficiency both *in vitro* and *in vivo*. The mRNA was delivered using an optimized LNP formulation, including ionizable lipid (Lipid 88 or ALC-0315), DSPC, DMG-PEG, and cholesterol. The S-specific immune response in spleen and lung induced by these new SARS-CoV-2 vaccines (TU88mCSA and ALCmCSA) were then evaluated in mice. The protection efficacy of these new vaccines was assessed in hamster model. DSPC, Distearoylphosphatidylcholine; DMG-PEG, 1,2-dimyristoyl-rac-glycero-3-methoxypolyethylene glycol-2000. Made in BioRender.

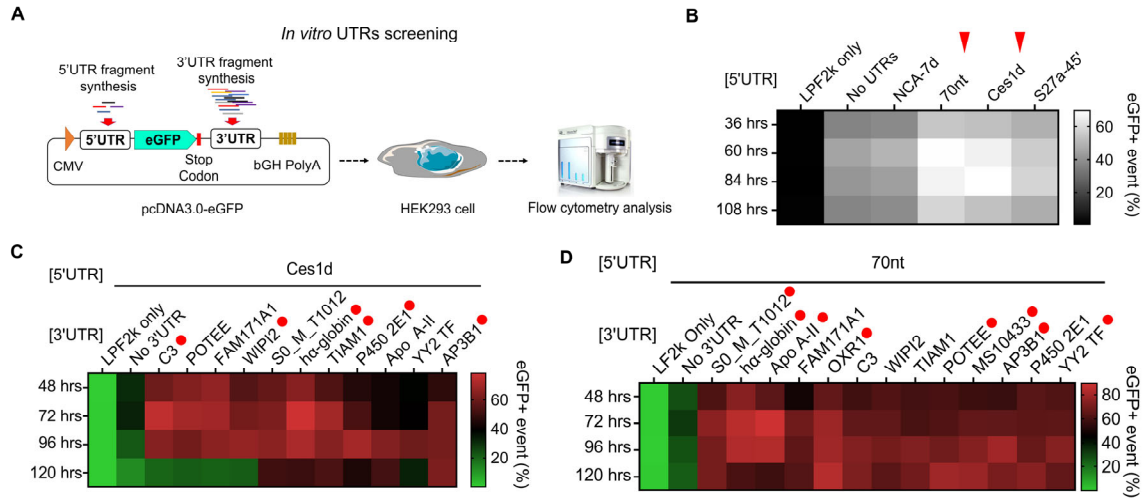


**Fig. S2. *In vitro* screening of UTRs.** (A) Schematic illustration of *in vitro* UTR screening. 5'UTR and 3'UTR fragments were introduced into a pcDNA3.0-eGFP backbone to evaluate the impact of each UTR sequence on eGFP expression in HEK293 cells. (B) Comparing the impact of 5'UTR fragments with each other on eGFP expression in HEK293 cells over time (36 hrs, 60 hrs, 84 hrs, and 108 hrs). Red arrows indicate the top-performed 5'UTRs (n=2). (C) Comparing the effect of 3'UTR fragments on pcDNA3.0-eGFP expression in HEK293 cells over time (48 hrs, 96 hrs, 108 hrs, and 120 hrs), using Ces1d as the 5'UTR. Red circles indicate the top-performed 3'UTRs (n=2). (D) Comparing the effect of 3'UTR fragments on pcDNA3.0-eGFP expression in HEK293 cells over time (48 hrs, 96 hrs, 108 hrs, and 120 hrs), using 70 nt as the 5'UTR. Red circles indicate the top-performing 3'UTRs. 500 ng plasmid was delivered using LPK2000 in each well (n=2).

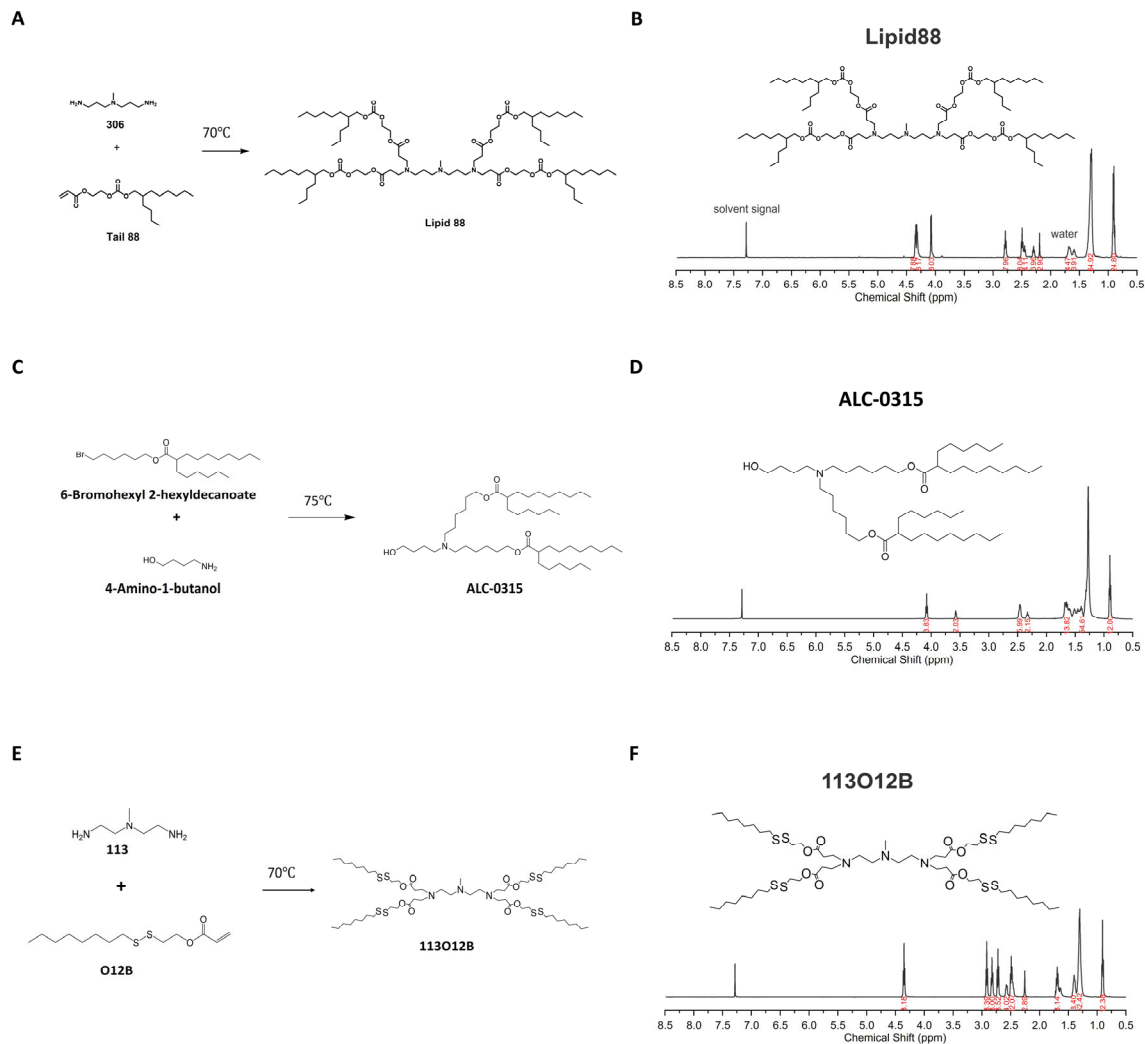


**Fig. S3. Synthesis and characterization of ionizable lipids: lipid88, ALC-0315 and 113O12B.** (A) Chemical synthesis of lipid88. (B) NMR of purified Lipid 88. (C) Chemical synthesis of ALC-0315. (D) NMR of purified lipid ALC-0315. (E) Chemical synthesis of 113O12B. (F) NMR of purified Lipid 113O12B.

### Supplementary Description (fig. S3)

#### <sup>1</sup>H nuclear magnetic resonance (<sup>1</sup>H NMR) spectra

Lipid88 NMR spectra (fig. S3B):

<sup>1</sup>H NMR (CDCl<sub>3</sub>, 500 MHz, ppm): δ 4,35 (m, J=5.0 Hz, 8H), 4.32 (m, J=5.0 Hz, 8H), 2.79 (t, J=10.0 Hz, 8H), 2.49 (t, J=10.0 Hz, 8H), 2.45 (t, J=10.0 Hz, 4H), 2.30 (t, J=10.0 Hz, 4H), 2.19 (s, 4H), 1.69 (m, J=5.0 Hz, 4H), 1.61 (m, J=5.0 Hz, 4H), 1.36–1.29 (m, 64H), 0.93-0.89 (m, 24H).

ALC-0315 NMR spectra (fig. S3D):

<sup>1</sup>H NMR (CDCl<sub>3</sub>, 500 MHz, ppm): δ 4,35 (m, J=5.0 Hz, 8H), 4.32 (m, J=5.0 Hz, 8H), 2.79 (t, J=10.0 Hz, 8H), 2.49 (t, J=10.0 Hz, 8H), 2.45 (t, J=10.0 Hz, 4H), 2.30 (t, J=10.0 Hz, 4H), 2.19 (s, 4H), 1.69 (m, J=5.0 Hz, 4H), 1.61 (m, J=5.0 Hz, 4H), 1.36–1.29 (m, 64H), 0.93-0.89 (m, 24H).

### 113012B NMR spectra (fig. S3F):

$^1\text{H}$  NMR ( $\text{CDCl}_3$ , 500 MHz, ppm): 4.35 (t, J=5.0 Hz, 8H), 2.92 (t, J=5.0 Hz, 8H), 2.82 (t, J=5.0 Hz, 8H),  $\delta$  2.72 (t, J=5.0 Hz, 8H), 2.58 (t, J=5.0 Hz, 4H), 2.51–2.45 (m, 12H), 2.26 (s, 3H), 1.69 (t, J=5.0 Hz, 8H), 1.40 (t, J=5.0 Hz, 8H), 1.34–1.27 (m, 32H), 0.93–0.89 (m, 12H).

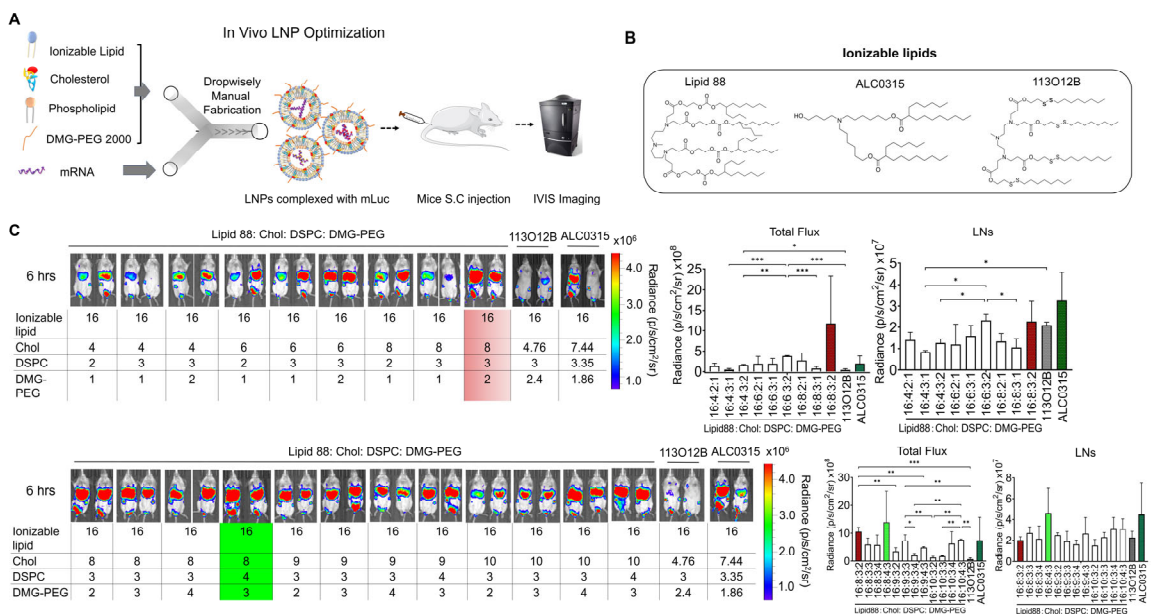


**Fig. S4. *In vivo* screening of top-performed LNP88 formulation via S.C route. (A)** Schematic illustration of *in vivo* LNP formulation optimization. For *in vivo* LNP optimization, the delivery efficiency for LNP88 formulations, 113012B and ALC-0315 was determined in mouse by quantifying firefly luciferase (Fluc) expression following tail-based subcutaneous (S.C.) injection, respectively. 5  $\mu\text{g}$  firefly luciferase mRNA (mLuc) was injected for each mouse. **(B)** Chemical structures of Lipid 88, ALC-0315, and 113012B used for LNP formulations in this study. **(C)** Quantified bioluminescence levels within the whole-body (total flux) and lymph nodes (LNs) under LNP88-mLuc, ALC-0315-mLuc, or 113012B-mLuc treatment at 6 hrs. LNP88 formulations were screened with a series of weight ratios of Lipid 88: Cholesterol: DSPC: DMG-PEG. Top-performing formulations are highlighted in brick red and green. Images of *in vivo* bioluminescence in mice at 6 hrs following S.C. injection of mLuc-LNPs are shown in the left panel. Unless specified otherwise, scale represents radiance (p/sec/cm<sup>2</sup>/sr) min=6.57e<sup>5</sup> to max=4.43e<sup>6</sup>. Significance was statistically determined by one-way ANOVA Tukey test, \*p<0.05, \*\*p<0.005, \*\*\* p<0.0005. Average  $\pm$  SD (n=2 mice per group), biological replicates shown.

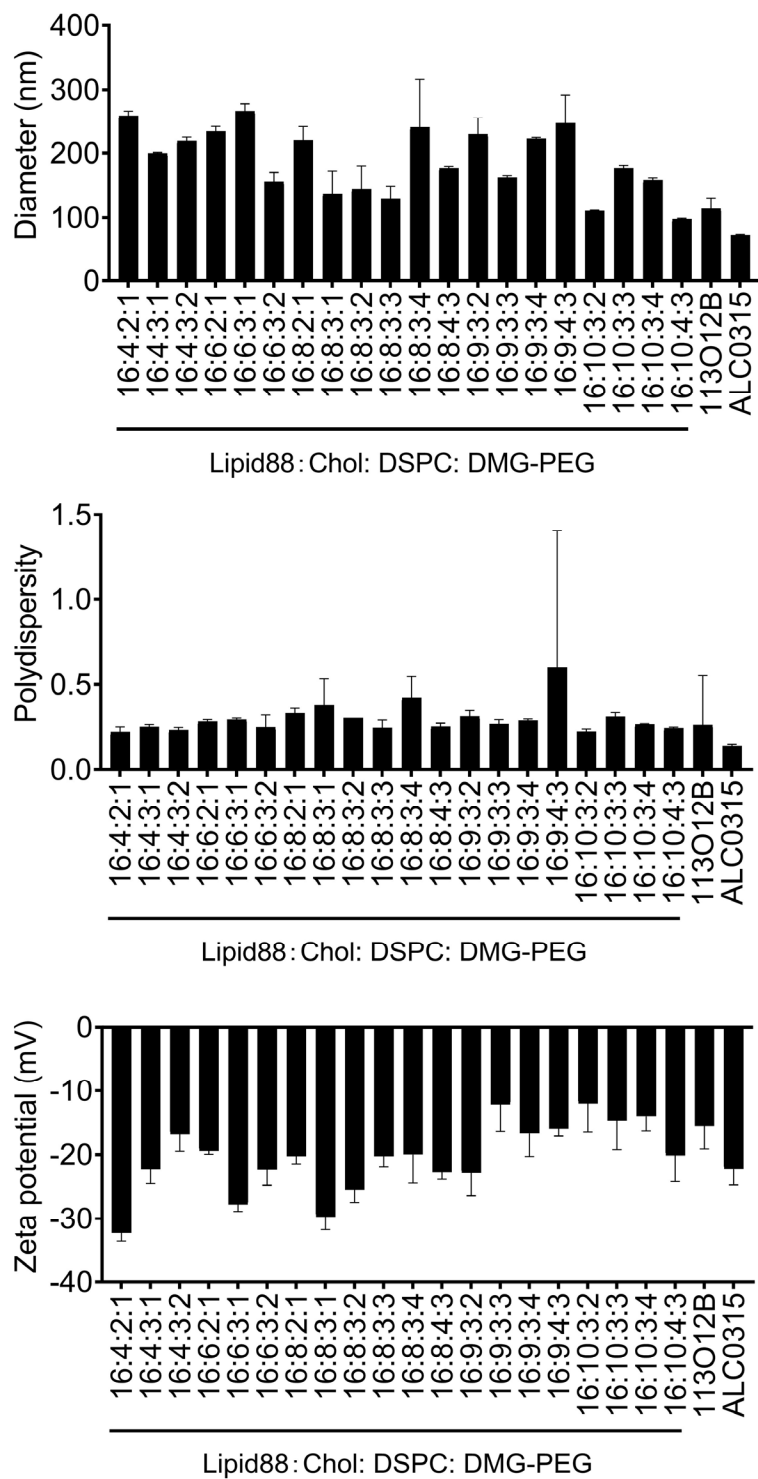


**Fig. S5. Physical properties of a series of LNP formulations used for S.C. LNPs-mLuc administration.** Various weight ratio of LNP88 formulations (lipid 88: Chol: DSPC: DMG-PEG) was studied. The effective diameter, polydispersity index and zeta potential of LNPs were then analyzed on DLS.

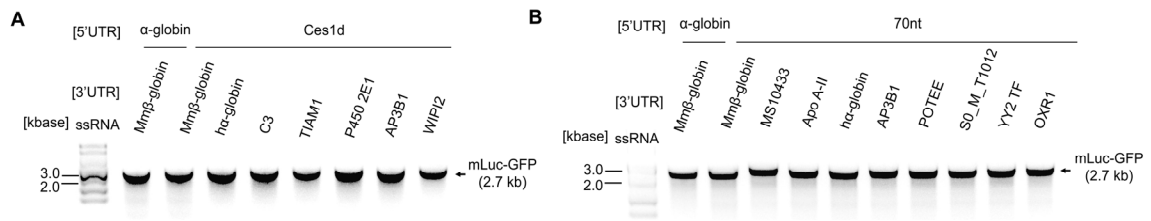


**Fig. S6. Gel electrophoresis of mRNA products. (A)** Quality control of mLuc-GFP containing a series of 3'UTR fragments (Mmβ-globin, ha-globin, C3, TIAM1, P450 2E1, AP3B1 or WIPI2) and a consistent 5'UTR (Ces1d). UTR combination (5'-α-globin-Mmβ-globin-3') from System Bioscience (SBI) was used as control. **(B)** Quality control of mLuc-GFP fused with a series of 3'UTR fragments (Mmβ-globin, MS10433, Apo A-II, ha-globin, AP3B1, POTEE, S0\_M\_T1012, YY2 TF or OXR1) and a consistent 5'UTR (70nt). UTR combination (5'-α-globin-Mmβ-globin-3') from SBI was used as control.

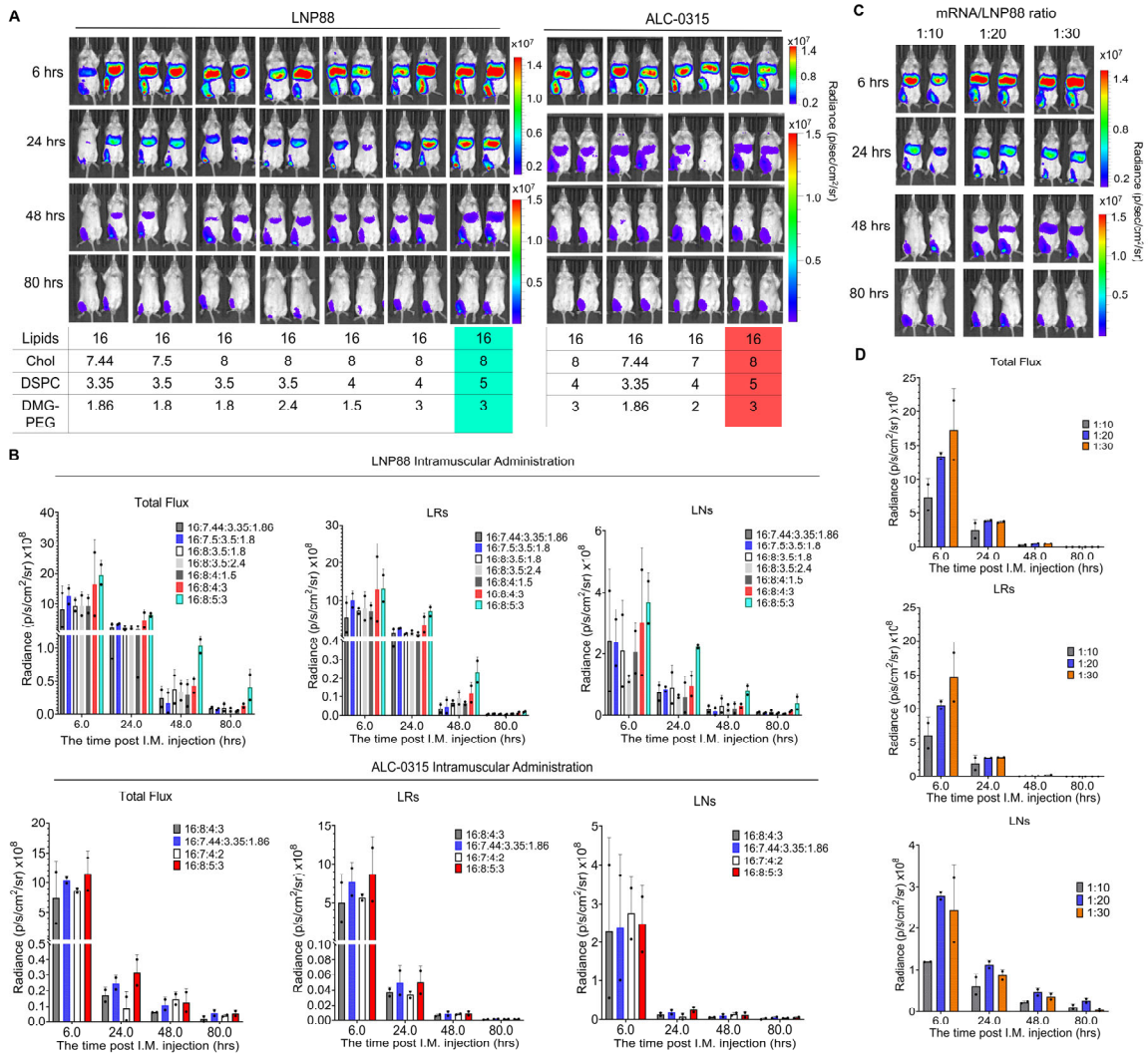


**Fig. S7. *In vivo* optimization of LNP88 and ALC-0315 formulations in mice *via* I.M. route. (A)** Images of *in vivo* bioluminescence measurements in mice at 6 hrs, 24 hrs, 48 hrs, and 80 hrs following I.M. injection of mLuc-LNP nanocomplex with a series of weight ratios of lipids: Chol: DSPC: DMG-PEG. Scale represents radiance (p/sec/cm<sup>2</sup>/sr), upper panel: min=1.0e<sup>6</sup> to max=1.5e<sup>7</sup>, and lower panel: min=1.0e<sup>5</sup> to max=1.5e<sup>7</sup>. **(B)** Quantification of bioluminescence over time in mice treated with mLuc loaded LNP88 or ALC-0315 nanocomplex. (n=2). **(C)** Images of *in vivo* bioluminescence measurements in mice at 6 hrs, 24 hrs, 48 hrs, and 80 hrs following I.M. injection of mLuc-LNP nanocomplex with a series weight ratio of mLuc to LNP88 (1:10, 1:20, 1:30) **(D)** Quantification of FLuc expression levels in mice with a series weight ratio of mLuc to LNP88 (1:10, 1:20, 1:30) from 6 hrs to 80 hrs after delivery. LR: Livers; LNs: lymph nodes. Scale represents radiance (p/sec/cm<sup>2</sup>/sr), upper panel: min=1.0e<sup>6</sup> to max=1.5e<sup>7</sup>, and lower panel: min=1.0e<sup>5</sup> to max=1.5e<sup>7</sup>. (n=2).

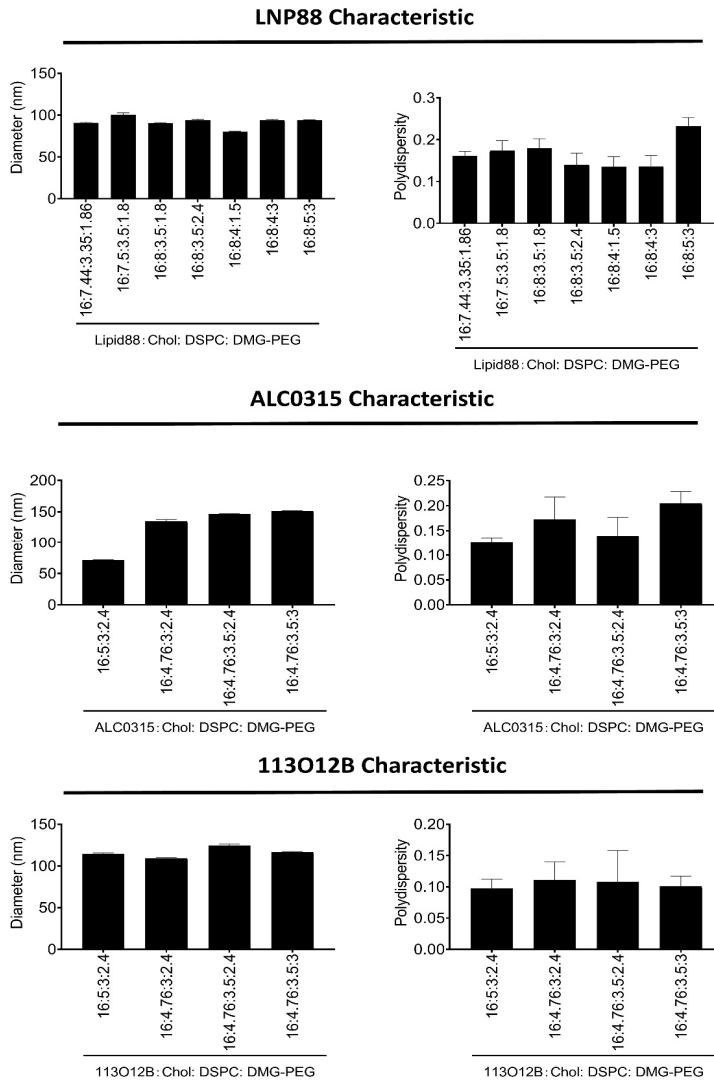


**Fig. S8. Physical properties of LNP88, ALC-0315 and 113O12B formulations used for mLuc delivery via I.M. administration.** Weight ratio of LNP formulations (active lipid: Chol: DSPC: DMG-PEG) was varied. The effective diameter, polydispersity index and zeta potential of each LNP were then analyzed on DLS.



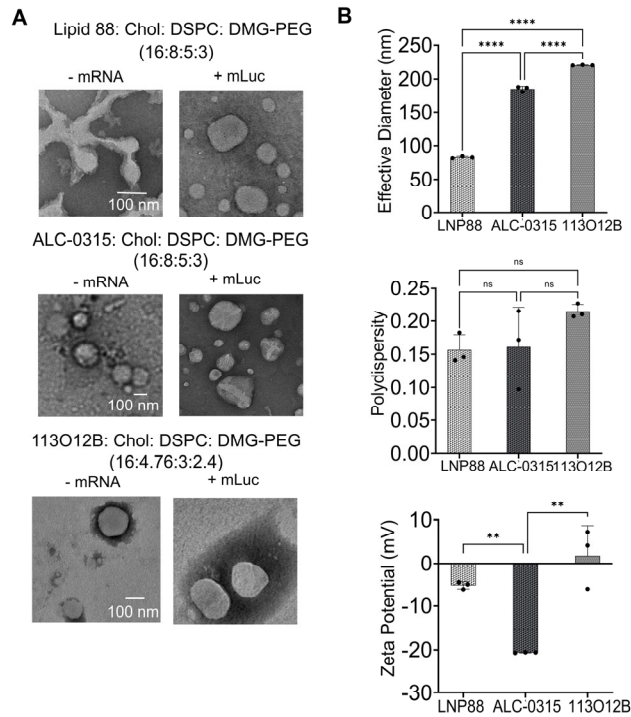


**Fig. S9. Physical properties of top-performed LNP88, ALC-0315 and 113012B LNP formulations used for I.M. LNPs administration. (A)** TEM images of the optimized LNP88, ALC-0315, and 113012B formulations with (right) and without (left) mLuc. Scale represents 100 nm. **(B)** DLS characteristics of the optimized LNP88, ALC-0315, and 113012B formulations without mRNA loading. Significance was statistically determined one-way ordinary ANOVA Tukey test, ns, no significance, \*\* $p < 0.005$ , \*\*\*\*  $p < 0.0001$ . Average  $\pm$  SD ( $n=3$ ).

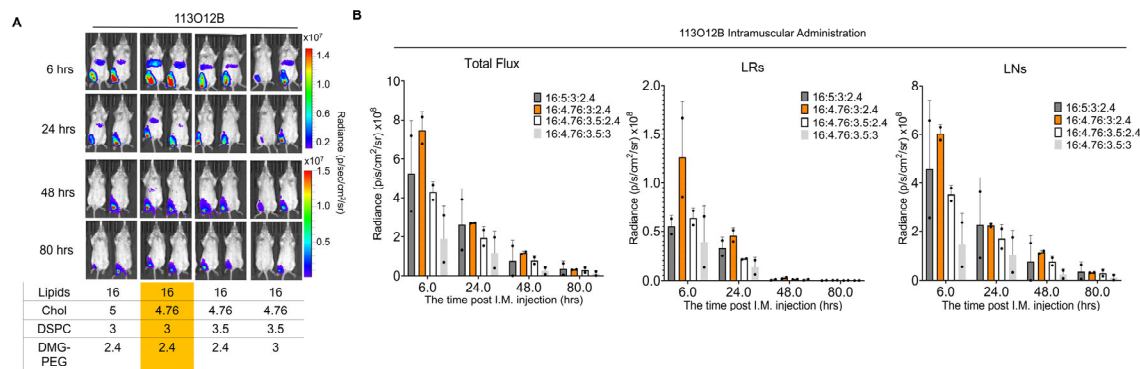


**Fig. S10. *In vivo* optimization of 113012B formulations in mice via I.M. route. (A)** Images of *in vivo* bioluminescence measurements in mice at 6 hrs, 24 hrs, 48 hrs, and 80 hrs following I.M. injection of LNP/mLuc nanocomplex with a series of weight ratios of active lipid: Chol: DSPC: DMG-PEG. Scale represents radiance (p/sec/cm<sup>2</sup>/sr), upper panel: min=1.0e<sup>6</sup> to max=1.5e<sup>7</sup>, and lower panel: min=1.0e<sup>5</sup> to max=1.5e<sup>7</sup>. **(B)** Quantification of bioluminescence over time in mice treated with 113012B /mLuc nanocomplex. ( $n=2$ ). LRs: Livers; LNs: lymph nodes.

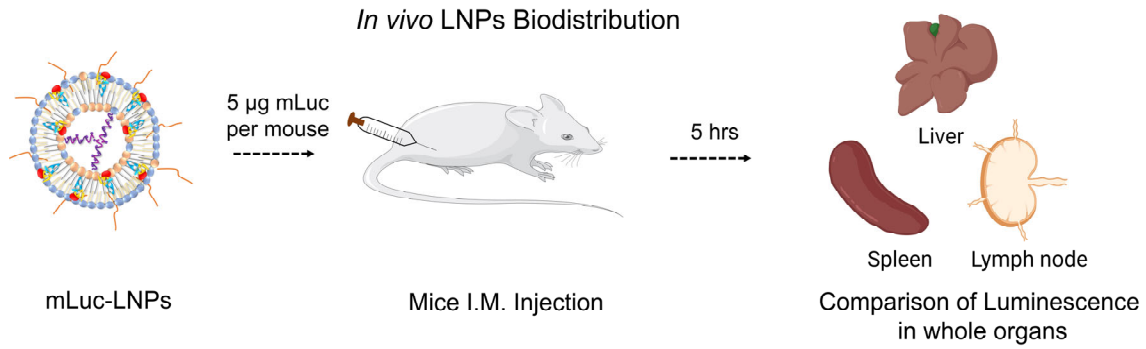


**Fig. S11. Schematic illustration of *in vivo* LNP-mediated mLuc delivery to specific organs in Balb/c mice.**

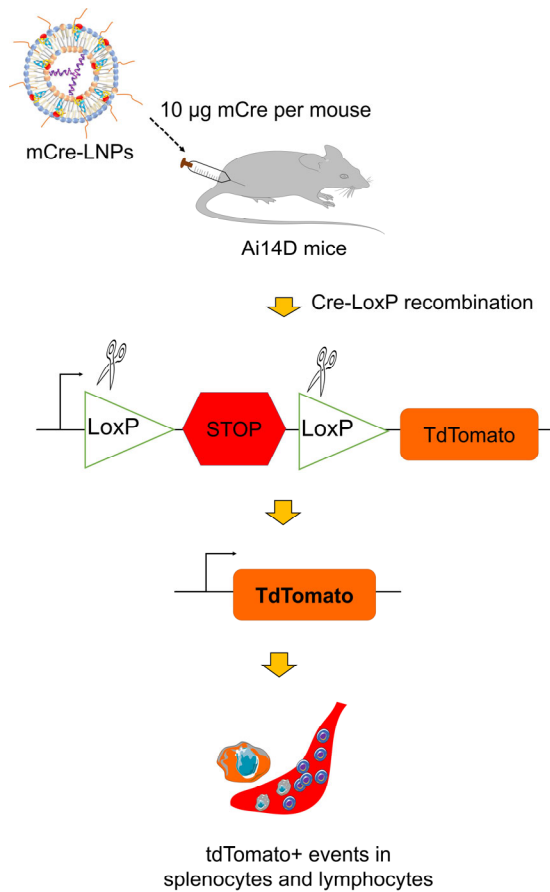


**Fig. S12. Schematic illustration of delivery of mCre-LNP88 or mCre-ALC-0315 through i.m. injection in tdTomato Ai14D mice.**

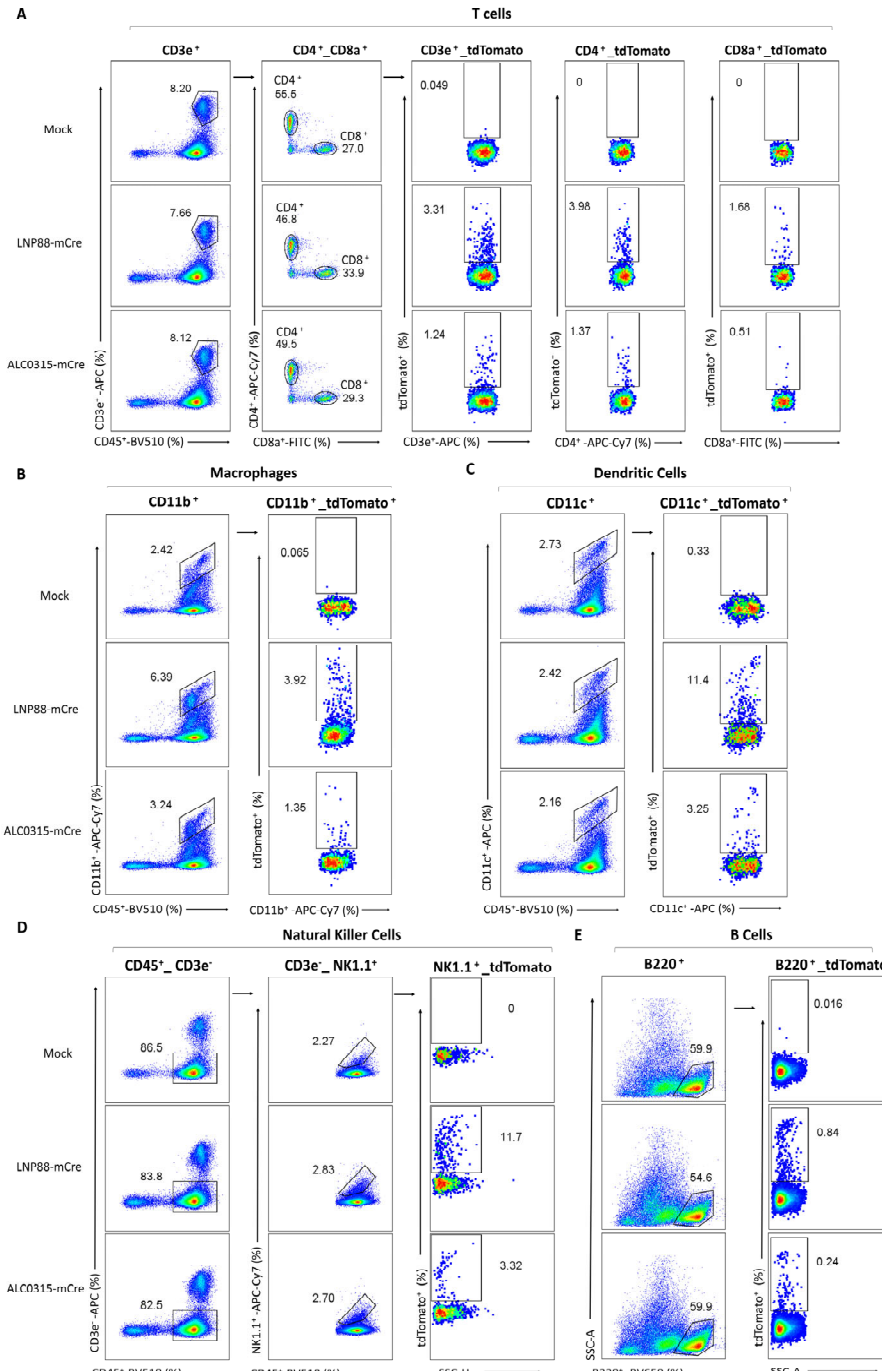


**Fig. S13. Subtypes of splenic immune cell analysis of LNPs-mediated mCre delivery in Ai14D mice at day 4 post i.m. injection. (A)** Flow cytometry measurement of tdTomato<sup>+</sup> expression in splenic CD3<sup>+</sup>, CD4<sup>+</sup> or CD8<sup>+</sup> T cells. **(B)** Flow cytometry measurement of tdTomato<sup>+</sup> expression in splenic CD11b<sup>+</sup> macrophages (Mφ). **(C)** Flow cytometry measurement of tdTomato<sup>+</sup> expression in splenic CD11c<sup>+</sup> dendritic cells (DC). **(D)** Flow cytometry measurement of tdTomato<sup>+</sup> expression in splenic CD3e-NK1.1<sup>+</sup> natural killer cells (NK). **(E)** Flow cytometry measurement of tdTomato<sup>+</sup> expression in splenic B220<sup>+</sup> B cells.

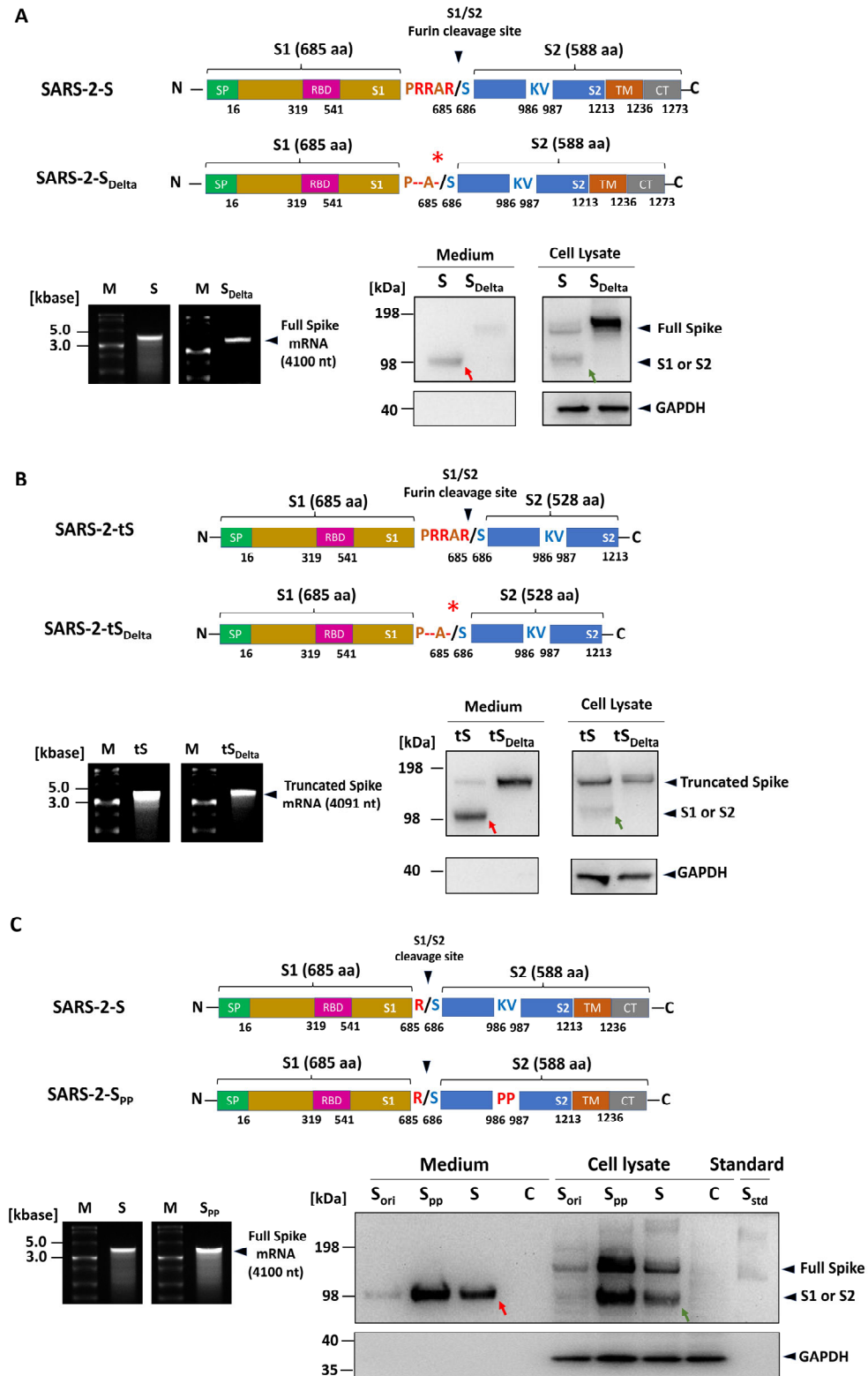


**Fig. S14. mRNA constructs of original spike protein and its variants, and their protein expression patterns in HEK293 cell culture. (A) Effect of furin cleavage site mutation on spike protein expression pattern. Original spike protein (SARS-2-S) with furin cleavage site led to shorter**

fragments (S1 or S2 fragment) in both culture medium and cell lysate fractions, suggesting that furin or TMPRSS2 (transmembrane protease, serine 2) on the membrane can access the S1/S2 site (PRRAR/S) and cleave the bond between arginine (R) and serine (S). Spike protein mutant with 3 Arginine (R) deletion close to the S1/S2 cleavage site (SARS-2-S<sub>delta</sub>, P--A-/S) abolished the furin cleavage site. The medium and cell lysate fractions did not produce either S1 or S2 fragments but full-length S<sub>delta</sub> was evidently detected in the cell lysate. **(B)** The effect of deletion of transmembrane domain (TM) and cytoplasmic tail (CT) on SARS-2-S and SARS-2-S<sub>delta</sub> leading to the expression of the secretory form of truncated spike protein. TM truncation in both SARS-2-S and SARS-2-S<sub>delta</sub> drove robust S2 fragment and full-length S<sub>delta</sub> into culture medium compared to untruncated SARS-2-S and SARS-2-S<sub>delta</sub>. GAPDH was used as the internal control. **(C)** The proline substitution at residues K986 and V987 on SARS-2-S and its expression pattern in HEK293 cells. Consistent with reported MERS and SARS2 S<sub>pp</sub>, two proline mutations augment S protein expression levels in HEK293 cells compared to both the original Wuhan-Hu-1 spike (S<sub>ori</sub>) and CDS optimized version (SARS-2-S). The band (red arrow) shown in the culture medium is S1 fragments and the lower band (green arrow) in cell pellet fraction are S2 fragments binding the cell membrane. SP, signal peptide; RBD, receptor-binding domain; Furin cleavage sites, S1-R/S-S2; TM, transmembrane domain; CT, cytoplasmic tail; Red arrows indicated S1 fragment and green arrow indicated S2 fragment.

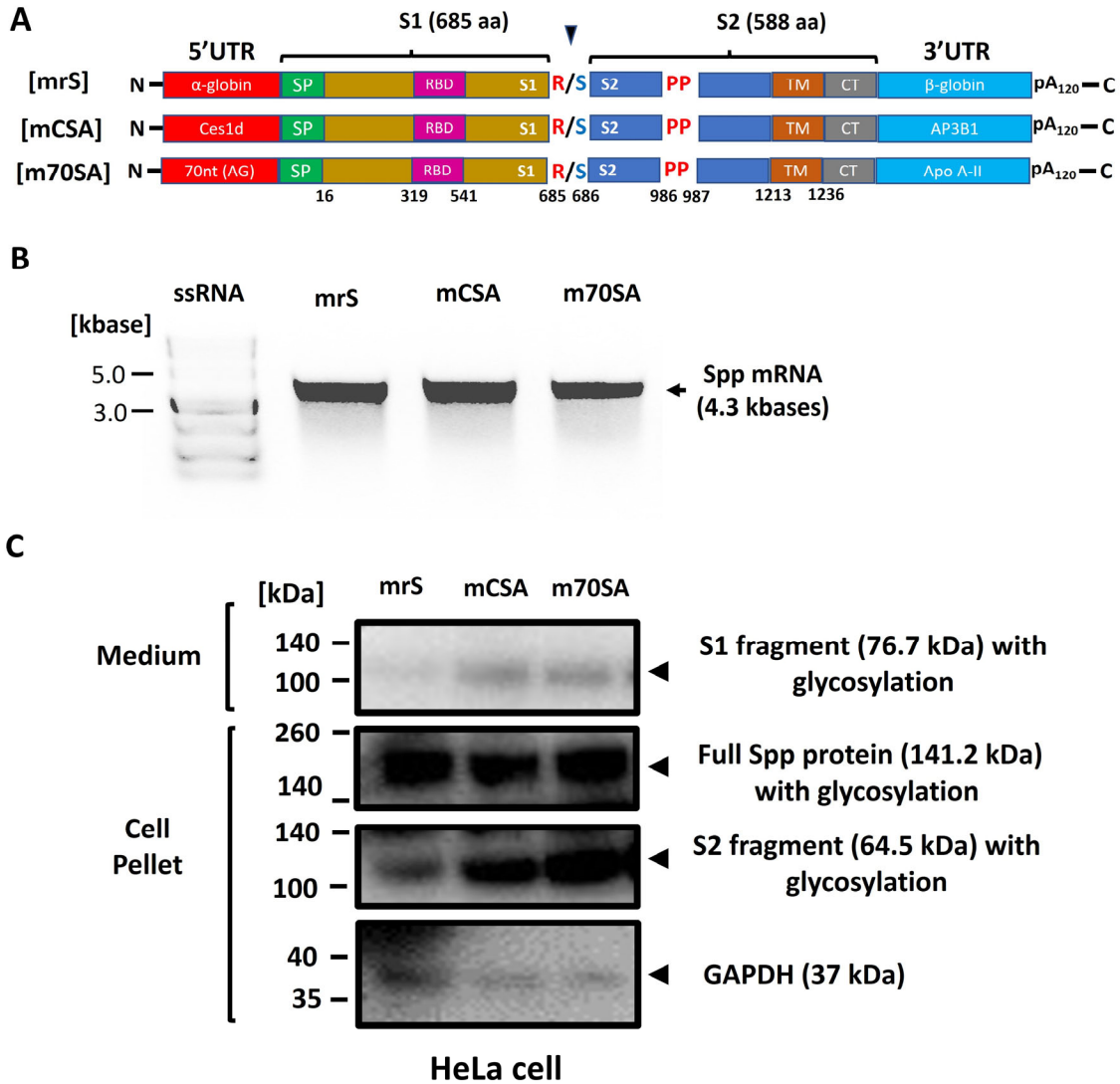


**Fig. S15. The effects of UTRs on spike mRNA translation in HeLa cells. (A)** Schematic illustration of full-length mammalian codon optimized SARS-CoV-2 spike gene with multiple UTRs combinations fusion. SP, signal peptide; RBD, receptor-binding domain; Furin cleavage sites, S1-R/S-S2; TM, transmembrane domain; CT, cytosol domain; Arrows indicate furin cleavage sites. **(B)** Gel electrophoresis of spike mRNA with different UTRs combination ( $\alpha$ -globin/M $\mu$  $\beta$ -globin, Ces1d/AP3B1, 70nt(AG)/Apo A-II). **(C)** Western blot of the spike protein expression in medium and cell lysate fractions of HeLa cells. S1 and S2 fragments and full length S<sub>pp</sub> were detected. This Semi-quantitative analysis showed that spike mRNA with Ces1d/AP3B1 and 70nt (AG)/Apo A-II UTR combinations increase protein expression comparing with mrS. GAPDH was used as the internal control.

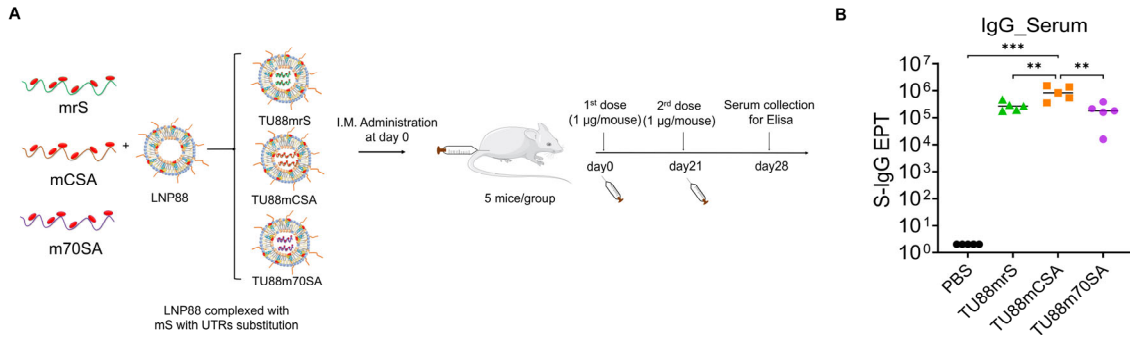
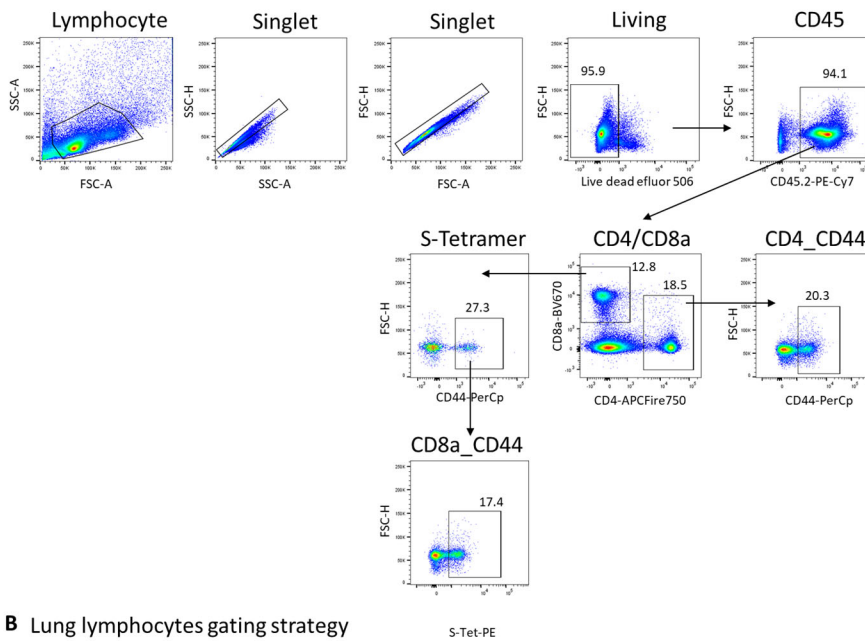


**Fig. S16. Serum S-specific IgG titer from mice immunized with three SARS-CoV-2 vaccine (TU88mrS, TU88mCSA and TU88m70SA).** **(A)** Schematic illustration of mice experimental design and timeline. Four groups of mice (n=5 per group) were vaccinated I.M. with mock (PBS), TU88mrS (1 µg), TU88mCSA (1 µg), and TU88m70SA (1 µg) at week 0 and 3. One week after booster vaccination (week 4), mice were euthanized and subjected to analysis of serum S-specific antibody response. **(B)** In ELISA measurements after booster (week 4) vaccination, the serum S-specific IgG end point titers (EPT) were compared between different vaccine groups. Significance for **B** was statistically determined by one-way ANOVA Tukey test, \*\* p<0.005, \*\*\* p<0.0005. Average ± SD (n=5 mice per group), biological replicates shown.

**A Spleen T cell gating strategy**



**B Lung lymphocytes gating strategy**

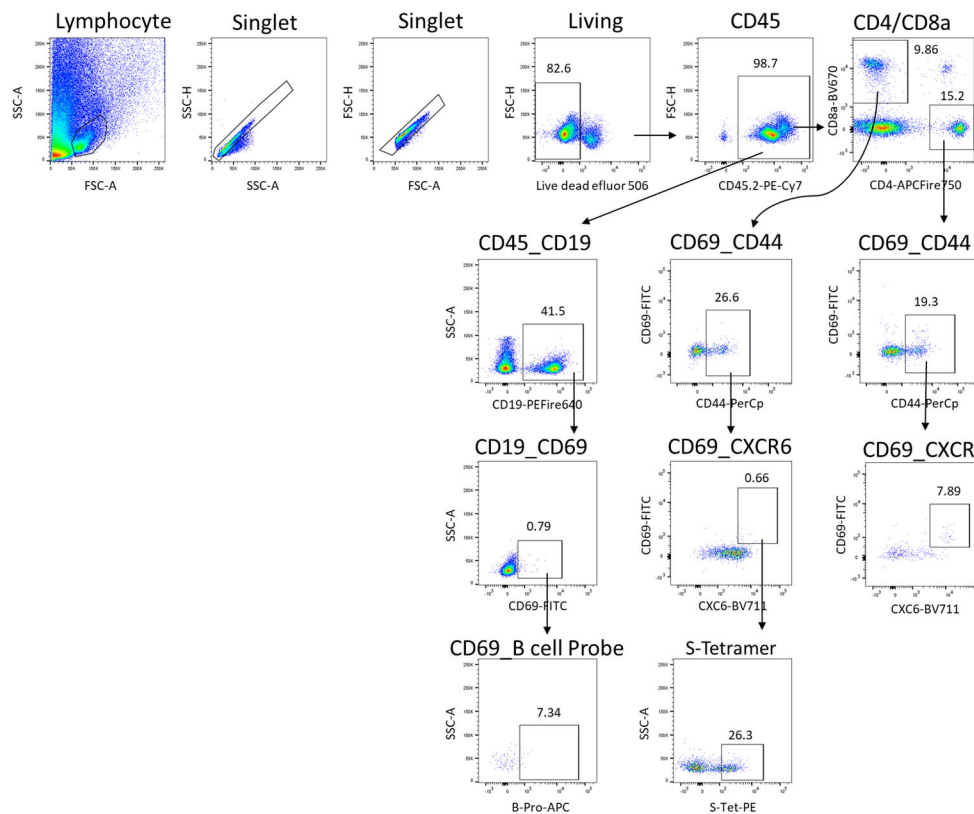


**Fig. S17. Representative T cells flow cytometry data from spleen and lung. (A)** Spleen naïve and activated T cells gating strategy. **(B)** Lung naïve and activated tissue resident T cells gating strategy. B cell probe, antigen probes for detection of SARS-CoV-2 spike-specific B cells. All other antibodies have been shown in Table S6.



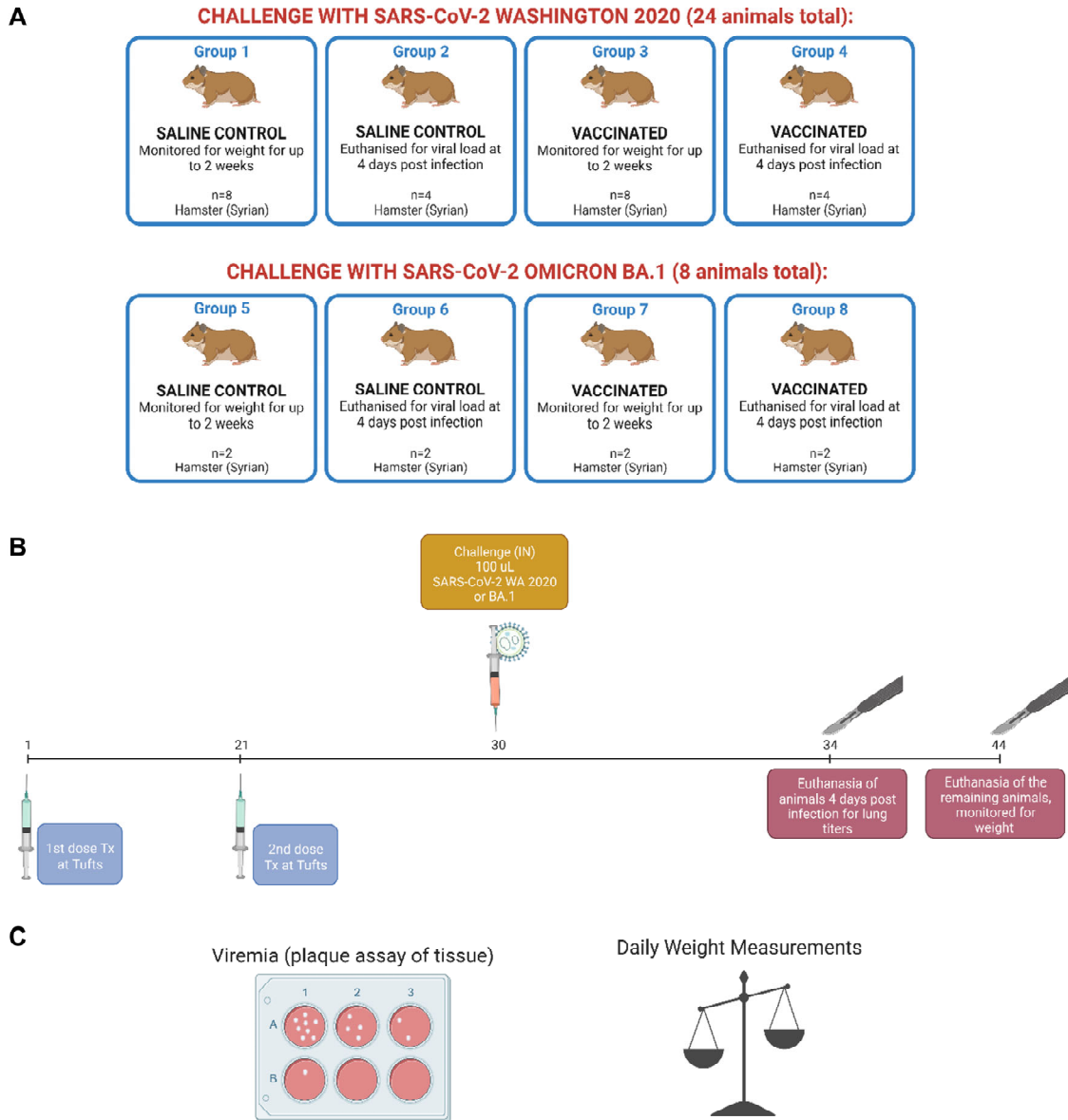
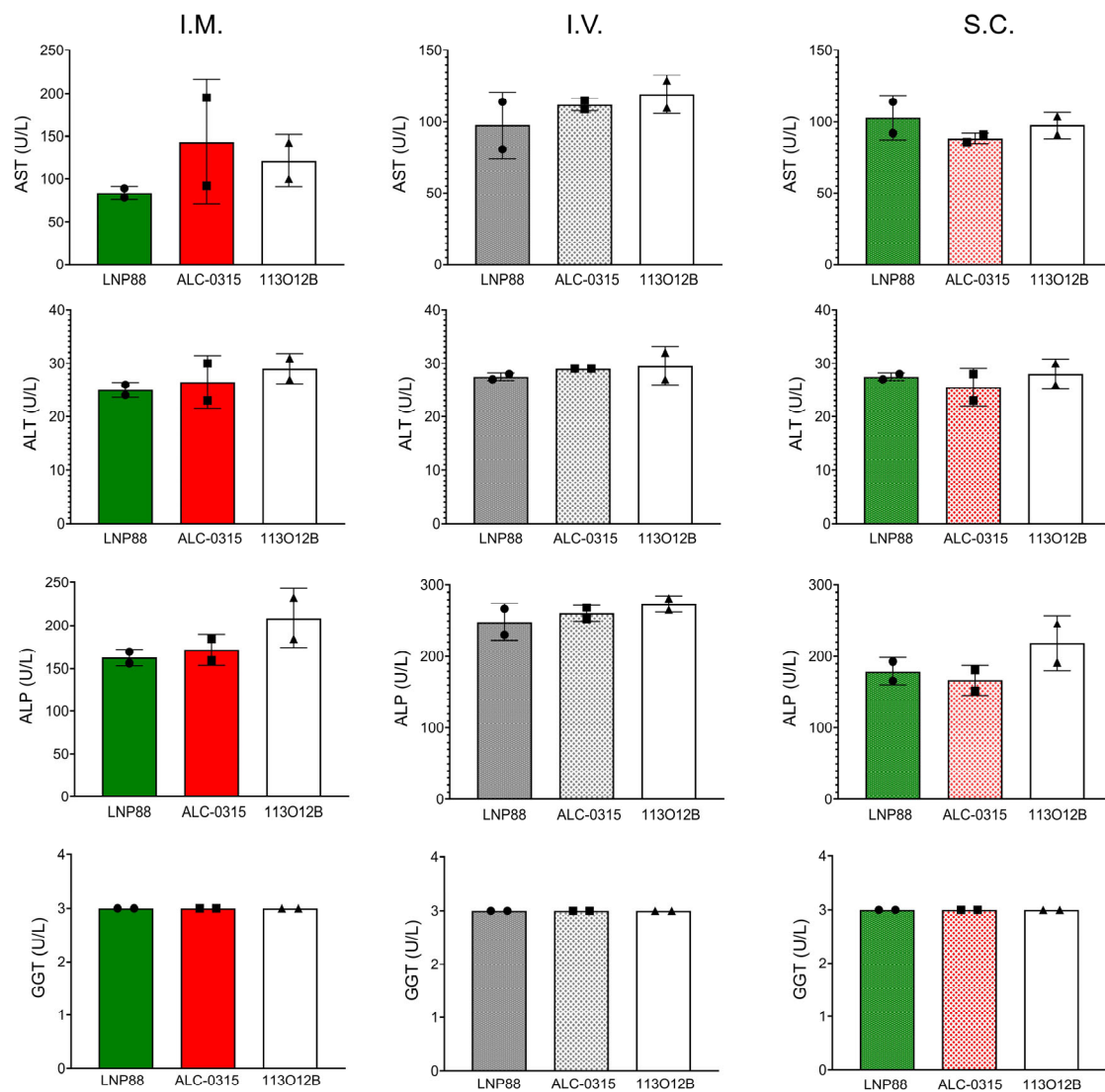


**Fig. S18. Visual timeline of *in vivo* Golden Syrian hamster immunization and SARS-CoV-2 viral challenge. (A)** Overview of treatment groups, divided into equivalent vaccinated and unvaccinated subgroups for viral challenge with SARS-CoV-2 WA 2020 (n=24) or Omicron BA.1 (n=8). **(B)** Timeline of two-dose TU88mCSA vaccination, viral challenge with WA 2020 / Omicron BA.1, and euthanasia of animals. **(C)** Schematic of study readouts including viremia as quantified by crystal violet plaque assay or daily weight measurements.

Day23  
(Day 2.5 post boost)



1 µg mRNA/30 µg LNP for each mice

Parameter	Units	Low	High
Alanine aminotransferase (ALT)	U/L	27	195
Alkaline phosphatase (ALP)	U/L	105	370
Aspartate aminotransferase (AST)	U/L	43	397
Gamma glutamyl transferase (GGT)	U/L	0.0	9.0

**Fig. S19. Measurement of systemic toxicity (liver function) in mice treated with mCSA-LNP at day 23 post 1<sup>st</sup> dose.** Levels of alanine aminotransferase (ALT), alkaline phosphatase (ALP), aspartate aminotransferase (AST), and gamma glutamyl transferase (GGT) in mice treated with 1 µg mCSA and 30 µg of LNP88, ALC-0135, or 113O12B via different administration (I.M., I.V. or S.C.).

Resulting slides were evaluated by the Study Pathologist, Sureshkumar Muthupalani, BVSc, MVSc, PhD, DACVP, according to the following parameters and corresponding scoring schemes:

- Inflammatory Infiltrate, Mixed Cell
- Vacuolation, Hepatocellular
- Vacuolation and Hypertrophy, Kupffer Cell
- Hepatocellular Necrosis, Coagulative
- Aggregates, Foamy/Vacuolated Macrophages
- Hepatocellular Single Cell Necrosis (Apoptosis)

**H&E Slide Evaluation**

- 0 Absent
- 1 Minimal
- 2 Mild
- 3 Moderate
- 4 Marked
- 5 Severe

Liver sections were also evaluated for increased hepatocellular mitotic activity, presence of multinucleated giant cells, vascular fibrin thrombi, and/or vascular necrosis. Bacteria (postmortem overgrowth or antemortem infection) were indicated when present in the tabulated data in Appendix A.

Scores for inflammatory infiltrate, mixed cell; vacuolation, hepatocellular; vacuolation and hypertrophy, Kupffer cells; aggregates, foamy/vacuolated macrophages; hepatocellular single cell necrosis; and hepatocellular necrosis, coagulative were added to calculate the cumulative pathology score for each liver section. Resulting tabulated microscopic data is presented in Appendix A.

**Appendix A**

2019-97		HISTOPATHOLOGY EVALUATION											
		0 = Absent; 1 = Minimal; 2 = Mild; 3 = Moderate; 4 = Marked; 5 = Severe; - = Tissue Normal											
Tissue	Route	Test Article	Group - Animal Identification	Inflammatory Infiltrate, Mixed Cell	Vacuolation, Hepatocellular	Vacuolation and Hypertrophy, Kupffer Cells	Aggregates, Foamy/Vacuolated Macrophages	Hepatocellular Single Cell Necrosis	Hepatocellular Necrosis, Coagulative	Cumulative Score	Bacteria - Post Mortem Overgrowth	Pathologist Comments	
Liver	Intramuscular	LNP88	PBS	1-1	0	0	0	0	0	0	0	-	Extensive tissue artifacts related to sub-optimal processing noted in all livers
			1-2	1	0	0	0	0	0	1	-		
	Empty LNP1	2-1	0	0	0	0	0	0	0	0	-		
		2-2	0	1	0	0	0	0	0	1	-		
	TU88mCSA	LNP3	3-1	0	0	0	0	0	0	0	-		
			3-2	1	0	0	0	0	0	1	-		
	ALCmCSA	LNP4	4-1	0	0	0	0	0	0	0	-		
			4-2	0	1	0	0	0	0	1	-		
	TU113mCSA	LNP5 (Pizer Lipid)	5-1	0	0	0	0	0	0	0	-		
			5-2	1	1	0	0	1	0	3	-		
	TU113mCSA	LNP6 (Pizer Lipid)	6-1	0	0	0	0	0	0	0	-		
			6-2	0	0	0	0	0	0	0	-		
	TU113mCSA	LNP7	7-1	1	0	0	0	1	0	2	-		
			7-2	1	0	0	0	0	0	1	-		
	TU113mCSA	LNP8	8-1	0	0	0	0	0	0	0	Moderate		
			8-2	0	0	0	0	0	0	0	-		

2019-97		HISTOPATHOLOGY EVALUATION											
		0 = Absent; 1 = Minimal; 2 = Mild; 3 = Moderate; 4 = Marked; 5 = Severe; - = Tissue Normal											
Tissue	Route	Test Article	Group - Animal Identification	Inflammatory Infiltrate, Mixed Cell	Vacuolation, Hepatocellular	Vacuolation and Hypertrophy, Kupffer Cells	Aggregates, Foamy/Vacuolated Macrophages	Hepatocellular Single Cell Necrosis	Hepatocellular Necrosis, Coagulative	Cumulative Score	Bacteria - Post Mortem Overgrowth	Pathologist Comments	
Liver	Intravenous	TU88mCSA	LNP9	9-1	1	0	0	0	1	0	2	-	
			9-2	0	0	0	0	0	0	0	-		
		ALCmCSA	LNP10	10-1	0	0	0	0	0	0	0	-	
				10-2	0	1	0	0	0	0	1	-	
		TU113mCSA	LNP11 (Pizer Lipid)	11-1	1	1	0	0	0	0	2	-	
				11-2	0	0	0	0	0	0	0	-	
		TU113mCSA	LNP12 (Pizer Lipid)	12-1	1	0	0	0	0	0	1	-	
				12-2	1	0	0	0	1	0	2	-	
		TU113mCSA	LNP13	13-1	1	0	0	0	0	0	1	-	
				13-2	1	0	0	0	0	0	1	-	
	TU88mCSA	LNP14	14-1	1	1	0	0	0	0	2	-		
			14-2	1	0	0	0	1	0	2	-		
	TU88mCSA	LNP15	15-1	1	0	0	0	1	0	2	-		
			15-2	1	0	0	0	0	0	1	-		
	ALCmCSA	LNP16	16-1	1	0	0	0	0	0	1	-		
			16-2	0	0	0	0	0	0	0	-		
	TU113mCSA	Subcutaneous	LNP17 (Pizer Lipid)	17-1	1	0	0	0	1	0	2	-	
				17-2	1	0	0	0	0	0	1	-	
	TU113mCSA	LNP18 (Pizer Lipid)	18-1	1	0	0	0	0	0	1	-		
			18-2	0	0	0	0	0	0	0	-		
TU113mCSA	LNP19	19-1	0	0	0	0	0	0	0	-			
		19-2	1	0	0	0	1	0	2	-			
TU113mCSA	LNP20	20-1	1	0	0	0	0	0	1	-			
		20-2	0	0	0	0	0	0	0	-			

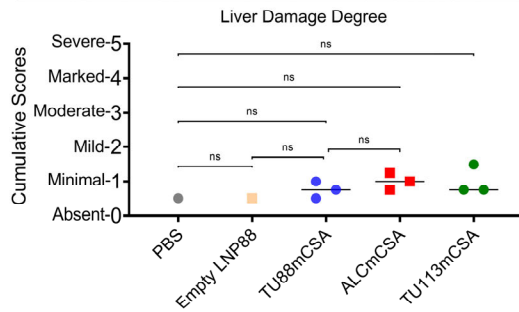


**Fig. S20. Pathology evaluation and scoring of systemic toxicity in liver of mouse treated with different mRNA formulations (TU88mCSA, ALCmCSA and TU113mCSA) and controls (30 µg blank LNP88 and PBS) via different routes of administration (I.M., I.V. and S.C.).** The dose of mRNA is 1 µg. At day 2.5 post 2rd dose, the toxicity of vaccines were evaluated by histopathology. All three administration routes were combined for each formulation, and the cumulative score was plotted.

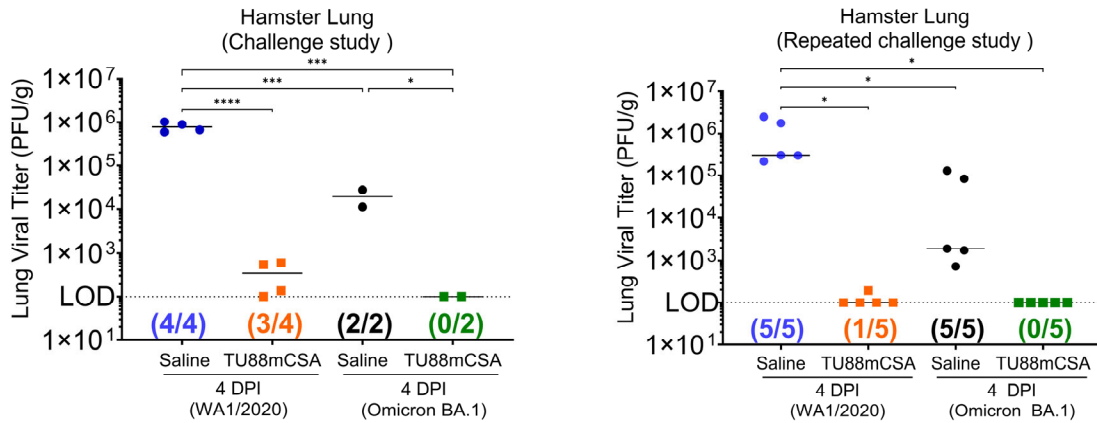


**Fig. S21. Reproducibility of the virus challenge study on vaccinated hamsters.** (Left) Lung viral titers from hamsters that were vaccinated with TU88mCSA (5 µg/hamster) or saline (control) and infected with WA1/2020 ( $4.0 \times 10^4$  pfu/hamster, n=4), or Omicron BA.1 ( $1.3 \times 10^4$  pfu/hamster, n=2). (Right) In a separate study, the lung viral titers from hamsters that were vaccinated with TU88mCSA (5 µg/hamster) or saline and infected with WA1/2020 ( $4.0 \times 10^4$  pfu/hamster, n=5) or with Omicron BA.1 ( $2.3 \times 10^4$  pfu/hamster, n=5). Significance was statistically determined by one-way ordinary ANOVA Tukey test, \*p<0.05, \*\*p<0.005, \*\*\* p<0.0005, \*\*\*\* p<0.0001. Average  $\pm$  SD. Biological replicates shown.

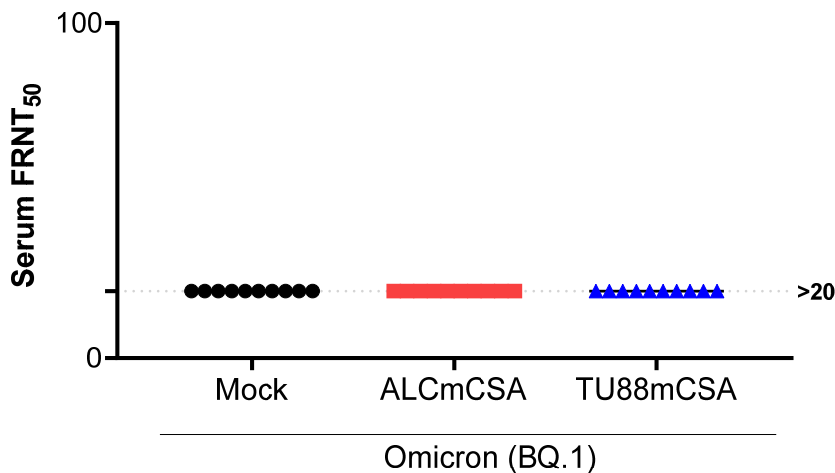


**Fig. S22. Neutralizing antibody titer in the hamsters prior to virus challenge.** Serum samples collected at week 5 after immunization were used to measure SARS-CoV-2 neutralizing titer by FRNT. FRNT<sub>50</sub> neutralization titers for individual serum samples were compared among different groups. Data were presented as median and IQR, and dotted lines are the LOD of the assay.

**Table S1:** Abbreviations and specific details of the key mRNA constructs and UTRs

Abbreviations	Specific details
TU88mCSA	Tufts-LNP88-Ces1d-S <sub>pp</sub> -AP3B1 [LNP: LNP88; mRNA construct: 5'UTR (Ces1d), CDS (S <sub>pp</sub> ) and 3'UTR (AP3B1)] with m <sup>1</sup> Ψ 100% incorporation
ALCmCSA	Acuitas-ALC-0315-Ces1d-S <sub>pp</sub> -AP3B1 [LNP: ALC-0315; mRNA construct: 5'UTR (Ces1d), CDS (S <sub>pp</sub> ) and 3'UTR (AP3B1)] with m <sup>1</sup> Ψ 100% incorporation
TU88mrS	Tufts-LNP88- <i>α</i> -globin-S <sub>pp</sub> - <i>β</i> -globin [LNP: LNP88; mRNA construct: 5'UTR ( <i>α</i> -globin), CDS (S <sub>pp</sub> ) and 3'UTR ( <i>β</i> -globin)] with m <sup>1</sup> Ψ 100% incorporation
ALCmrS	Acuitas-ALC-0315- <i>α</i> -globin-S <sub>pp</sub> - <i>β</i> -globin [LNP: ALC-0315; mRNA construct: 5'UTR ( <i>α</i> -globin), CDS (S <sub>pp</sub> ) and 3'UTR ( <i>β</i> -globin)] with m <sup>1</sup> Ψ 100% incorporation
<i>hα</i> -globin	human <i>α</i> -globin (Table S3)
FAM171A1	Astroprincin (Table S3)
POTEE	prostate, ovary, testis, and placenta expressed ankyrin domain family member E (Table S3)
C3	complement component 3 (Table S3)
WIPI2	WD Repeat Domain, Phosphoinositide Interacting 2 (Table S3)
P450 2E1	cytochrome P450 family 2 subfamily E member 1 (Table S3)
Apo A-II	Apolipoprotein (Table S3)
Ces1d	Carboxylesterase 1d (Table S3)
AP3B1	adaptor protein-3β (Table S3)

**Table S2:** 5'UTR sequences used for this project.

5'UTR	Fragment Sequence*
S27a-45'	CCACTAGTTCTAGAGGTACCTTGGACCCTCGTACAGAAGC <b>TAATACGACTCA</b> <b>CTATA</b> GGGAGGAAAGAATCGCATCGGCTGTATAAGAAAGCCTTTTGAGGCAT TTTTTTTAGTTGAGCACATCATTTGAGGCCATTCTGAGGTAACCGAGAAAA GAGCGTAAAGAAACCGAGCGAACGAGCAAATCTGGCACTGCGTTAGACAGC CGCGATTCCGCTGCAGCGCGCAGGCACGTGTGTGGCCGCCTAAGGGGCGG GTCCTTCGGCCAGGAGACCCCGTCCGCCACGCTCGGATCTTCTTTCCGAT CCGCCATCGTGGGTGGAGCCGCCGACC <b>GAATTC</b> GCCACCATGGAAGA
NCA	CCACTAGTTCTAGAGGTACCTTGGACCCTCGTACAGAAGC <b>TAATACGACTCA</b> <b>CTATA</b> GGCAAAAATCAAATCAATCATCATCACAAACATCAACAATCAATCATC AACACATCATCAAGACACCACC <b>GAATTC</b> GCCACCATGGAAGA
70nt or 70nt (GG)	CCACTAGTTCTAGAGGTACCTTGGACCCTCGTACAGAAGC <b>TAATACGACTCA</b> <b>CTATA</b> GGGAAGAGATAAACATAAACATAAACGACAAGAAACACATACAAAAG AAACAGGACAGAAAACAGCCACC <b>GAATTC</b> GCCACCATGGAAGA
Ces1d	CCACTAGTTCTAGAGGTACCTTGGACCCTCGTACAGAAGC <b>TAATACGACTCA</b> <b>CTATA</b> AGGAGGCGGGTCCCCTGGTCCACAACAGAAGCATTGCTAAAGCAGC AGATAGCTCAGAGACCCACAGAGCCCTTGTCTTCCACA <b>GAATTC</b> GCCACC ATGGAAGA
70nt (AG)	CCACTAGTTCTAGAGGTACCTTGGACCCTCGTACAGAAGC <b>TAATACGACTCA</b>

CTATAAGGAAGAGATAAACATAAACATAAACGACAAGAAACACATACAAAAGA  
AACAGGACAGAAAACAGCCACCGAATTCGCCACCATGGAAGA

a-globin  
(SBI) TAATACGACTCACTATAGGGAAATAAGAGAGAAAAGAAGAGTAAGAAGAAAT  
ATAAGA

*\*Homologous regions are underlined. The T7 promoter is highlighted in green. Each fragment is highlighted in yellow. First 2 bases are marked in red. Restriction enzyme cutting sites are in bold.*

**Table S3:** 3'UTR sequences used for this study.

3'UTR	Fragments Sequence*
XbaI-Moderna 3'UTR (a-globin)-ApaI	<u>AGCTGTACAAGTAATCTAGAGCTGGAGCCTCGGTGGCCTAGCTT</u> <u>CTTGCCCCTTGGGCCTCCCCCAGCCCCTCTCCCCTTCTGCA</u> <u>CCCGTACCCCGTGGTCTTTGAATAAAGTCTGAGTGGGCGGCAG</u> <u>GGCCCTATTCTATAGTGTC</u>
XbaI-Pfizer 3'UTR (MS10433)-ApaI	<u>AGCTGTACAAGTAATCTAGACTCGAGCTGGTACTGCATGCACGCA</u> <u>ATGCTAGCTGCCCCTTTCCCGTCCCTGGGTACCCCGAGTCTCCCC</u> <u>CGACCTCGGGTCCCAGGTATGCTCCACCTCCACCTGCCCACT</u> <u>CACCACCTCTGCTAGTTCCAGACACCTCCCAAGCACGCAGCAAT</u> <u>GCAGCTCAAACGCTTAGCCTAGCCACACCCCCACGGGAAACAG</u> <u>CAGTGATTAACCTTAGCAATAAACGAAAGTTAACTAAGCTATAC</u> <u>TAACCCAGGGTTGGTCAATTCGTGCCAGCCACACCCTGGAGC</u> <u>TAGCGGGCCCTATTCTATAGTGTC</u>
XbaI-Apolipoprotein A-II 3'UTR-ApaI	<u>AGCTGTACAAGTAATCTAGAAGTGTCCAGACCATTGTCTTCCAAC</u> <u>CCCAGCTGGCCTCTAGAACCCCACTGGCCAGTCTTAGAGCTCC</u> <u>TGTCCCTACCCACTTTTGCTACAATAAATGCTGAATGAATCCAG</u> <u>GGCCCTATTCTATAGTGTC</u>
XbaI-Cytochrome P450 2E1 3'UTR- ApaI	<u>AGCTGTACAAGTAATCTAGAGTGTGTGGAGGACACCCTGAACCC</u> <u>CCCGCTTTCAAACAAGTTTTCAAATTGTTTGAGGTCAGGATTTCTC</u> <u>AAACTGATTCTTTCTTTGCATATGAGTATTTGAAAATAAATATTTT</u> <u>CCCAGAATATAAATAAATCATCACATGATTATTTAACTATGGGCC</u> <u>CTATTCTATAGTGTC</u>
XbaI-Complement Component 3 3'UTR- ApaI	<u>AGCTGTACAAGTAATCTAGACCACACCCCACTCCCACTCCAG</u> <u>ATAAAGCTTCAGTTATATCTCACGTGTCTGGAGTTCTTTGCCAAGA</u> <u>GGGAGAGGCTGAAATCCCAGCCGCCTCACCTGCAGCTCAGCTC</u> <u>CATCCTACTTGAAACCTCACCTGTTCCACCGCATTCTCCTGG</u> <u>CGTTCGCCTGCTAGTGTGGGGCCCTATTCTATAGTGTC</u>
XbaI-YY2 Transcription Factor 3'UTR-ApaI	<u>AGCTGTACAAGTAATCTAGAGTATTTTCTGCTTAAAAAAGTTATA</u> <u>TAGGTGTTATTTGTTTTAATCTTGGTTGTAGTCTTGGATGTTAACA</u> <u>CATCTTGCAATTTAGCTGTATTAGGTCATGTAGTATTGATATTAGG</u> <u>TGATTTAATAGTACTAGTTTAAACCTATTTTAGTCATTTTATGGGCC</u> <u>CTATTCTATAGTGTC</u>
XbaI-TIAM1 3'UTR- ApaI	<u>AGCTGTACAAGTAATCTAGACGCCTTTCGGGTTCCAGGGCTTCG</u> <u>AGCTTGATCTTTTAAAAGTTTTATTCTATTAATTTTTGCTATATCT</u> <u>TCTGGTTTTCTGAAAAGCTTTAGAATGGTTTCTATACCCTTTGTA</u> <u>TCACTGCATTTTCCATATCATCTCCGGTTCGATCGCGTCCAGGG</u> <u>CCCTATTCTATAGTGTC</u>
XbaI-FAM171A1 3'UTR-ApaI	<u>AGCTGTACAAGTAATCTAGAAAAGCTGTCGTTGAGAACTTAGGTTG</u> <u>GCACGTAGCGTCTCAAGGTATGCGTTCTCTCAAAGGAAAGCTATG</u> <u>CATCGCTGCTTCGTTGCTGATTTTGCTTAGATTTTGCTTTGGTTA</u> <u>GGTTGCGTTTTGGGGTTTTGCCTTTTTTTGTTGTCGCTTAAATGCG</u> <u>GGCCCTATTCTATAGTGTC</u>

XbaI-AP3B1 3'UTR- ApaI	<u>AGCTGTACAAGTAATCTAGAAGAATGCTAGTGTGTATCTATCATGT</u> ATGCAATACTTTCCCCCTTTTTGCTTTGCTAACCAAAGAGCATATA TTTTACTGTCAGTTGTCTCAACTCTTGAATCCATGTGGCGTTTTCT CTGTCCTGCTGCTTCTTTTGGCCTCCTCGTTTTCTTCTCTTGGG CCCTATTCTATAGTGTC
XbaI-OXR1 3'UTR- ApaI	<u>AGCTGTACAAGTAATCTAGAGCAATACAGTGTAAACATGTCACTTG</u> TGCTTTAAAATTAGTCTGTATCACCATTTATTACAGTTATAATTTTG GAGTTTATTTTTCAAATCATGTTCTTGTCCCAGAGTTCTTTAGGTT AACACTAGGGACTGCGTCCATGTAAGTATAACAGCTTGGGGG GCCCTATTCTATAGTGTC
XbaI-POTEE 3'UTR- ApaI	<u>AGCTGTACAAGTAATCTAGATGGCCCAGTCCTCTCCCTAGTTCAC</u> ACAGGGGAGGTGATAGCATTGCTTTTGTGCAAATTACATAATGCA AAATTTTTGAATCTTGCCTTAATACTTTTTAATTTGTTTTATTTT GAATGATCAGCCTTCGTGGCCCCCTCTTTTGTACCCCACTGG GCCCTATTCTATAGTGTC
XbaI-WIPI2 3'UTR- ApaI	<u>AGCTGTACAAGTAATCTAGAATCCTGCTTATGAATTTTAGCTTTTT</u> GTTTGTGTTGTTTTCTTTTTGCCAAAATTAAGTGTGGTGAAGC CCGCAAACCTCCTCGCTTTGCATGCATGAACGTGCCAAGCCAG CATAGGGGAGCTAGAAGCCACTTTCCAGCCACCTGCCGTTGGGT GGCCCTATTCTATAGTGTC
XbaI-S0_M_T1012 3'UTR-ApaI	<u>AGCTGTACAAGTAATCTAGACGACTATTTAAACAGACTGTTTTAAT</u> CTGTGAAAATGGTTGGTAACTGTGAAAATAAGATACTGTGGATA TCTAACCAATCGCACTTAACGACTCGGGCCACCACTGTCCGGCC CTATTCTATAGTGTC
Mmβ-globin (SBI)	GCTGCCTTCTGCGGGGCTTGCCTTCTGGCCATGCCCTTCTTCTCT CCCTTGACCTGTACCTCTTGGTCTTTGAATAAAGCCTGAGTAGG AAG

*\*Homologous regions are underlined. Xba1 and Apa1 were added the two ends of each 3'UTR fragment.*





**A224**      **CCACTAGTTCTAGAGGTACC**  
**A225**      **TCTTCATGGTGGCGAATTC**  
**A333**      **AGCTGTACAAGTAATCTAGA**  
**A334**      **GACACTATAGAATAGGGCC**  
**A348**      **CCACTAGTTCTAGAGGTACC**  
**A349**      **TTACTTGTACAGCTCGTCCA**  
**A350**      **AGCTGTACAAGTAATCTAGA**  
**A351**      **tttttttttttaaatattGACACTATAGAATA**

---

\*: Overlapping region for expected mutations are shown as red nucleotides. The underlined long primer arm fuses with EcoRI and BamHI-digested pMRNAxp vector by Cold Fusion recombination.

**Table S5:** Antibodies used for immune cells subtyping on Ai14D mice

Marker	Label	Manufacturer	Catalog#
CD45	Brilliant Violet 510	BD Biosciences	BDB563891
CD3e	APC	Invitrogen	17003181
CD8a	FITC	BioLegend	100706
CD4	APC-Cy7	BD Biosciences	BDB561830
F4/80	eFluor660	Invitrogen	50-4801-82
CD11b	APC/Cy7	BioLegend	101225
CD11c	APC	Invitrogen	17011481
B220	Brilliant Violet 650	BD Biosciences	BDB563893
NK1.1	APC-Cy7	BD Biosciences	BDB560618

**Table S6:** Antibodies used for spleen and lung S-specific T cells subtyping on C57BL/6 mice

Marker	Label	Source	Catalog#
CD45	PE/Cyanine7	Biolegend	109830
CD4	APC/Fire™ 750	Biolegend	100460
CD8a	Brilliant Violet 570™	BioLegend	100740
CD44	APC-Cy7	Biolegend	103036
CD69	eFluor660	BD Pharmingen™	553236
CD186 (CXCR6)	Brilliant Violet 711™	BioLegend	151111
CD19	PE/Fire™ 640	Biolegend	115574
CD3	APC	Biolegend	100236
eBioscience™ Fixable Viability Dye	eFluor™ 506	Invitrogen™	65-0866-14
S539–546 epitope–specific CD8+ T cell	PE	National Institutes of Health (NIH) Tetramer Core	
Recombinant RBD protein coupled with allophycocyanin	APC	A kind gift from Dr. Jie Sun, Carter Immunology Center, University of Virginia, Charlottesville, VA 22908, USA.	

## References:

1. J. Chen et al., Lipid nanoparticle-mediated lymph node-targeting delivery of mRNA cancer vaccine elicits robust CD8(+) T cell response. Proc. Natl. Acad. Sci. U.S.A. 119, e2207841119 (2022).